Electronic Supplementary Material (ESI) for ChemComm.

Electronic Supplementary Information

Carba-*closo*-dodecaboranylethynyl ligands facilitating luminescent reversed charge-transfer excited states in gold/silver complexes

Michael Hailmann,[a] Benjamin Hupp,[b] Alexander Himmelspach,[a] Fabian Keppner,[a]
Philipp T. Hennig,[a] Rüdiger Bertermann,[a] Andreas Steffen*[b] and Maik Finze*[a]

Institut für Anorganische Chemie, Institut für nachhaltige Chemie & Katalyse mit Bor (ICB), Julius-Maximilians-Universität Würzburg, Am Hubland, 97074 Würzburg, Germany.
E-Mail: maik.finze@uni-wuerzburg.de.
Homepage: https://go.uniwue.de/finze-group

Fakultät für Chemie und Chemische Biologie, Technische Universität Dortmund, Otto-Hahn-Str. 6, 44227 Dortmund, Germany.
andreas.steffen@tu-dortmund.de

Experimental Section

^{1}H, ^{11}B, ^{13}C and ^{31}P NMR spectra were recorded at 25 °C either in CD_2Cl_2 or $(CD_3)_2SO$ on a Bruker Avance 500 or on a Bruker III HD 300 spectrometer. The NMR signals were referenced against TMS (^{1}H and ^{13}C), $BF_3 \cdot OEt_2$ in $CDCl_3$ with $\Xi(^{11}B) = 32.083974$ MHz, and 85% orthophosphoric acid (H_3PO_4) with $\Xi(^{31}P) = 40.480742$.[1] The assignment of the ^{11}B and ^{1}H signals is aided by $^{11}B\{^{1}H\}$-$^{1}H\{^{11}B\}$ 2D,[2, 3] $^{11}B\{^{1}H\}$-$^{1}H\{^{11}B\}$ COSY[4, 5] and $^{1}H\{^{11}B_{selective}\}$ experiments. Solid-state $^{11}B\{^{1}H\}$ MAS rotor-synchronized Hahn-echo (RSHE) and $^{31}P\{^{1}H\}$ VACP/MAS NMR spectra were recorded at 22 °C with a Bruker DSX-400 NMR spectrometer with bottom layer rotors of ZrO_2 (diameter 4 mm) containing approximately 30–50 mg of sample (^{11}B, 128.38 MHz; ^{31}P, 161.98 MHz). The measurements were conducted with a spinning rate of 15 kHz. All chemical shifts were calibrated by setting the ^{13}C low-field signal of adamantane to $\delta = 38.48$ ppm according to the IUPAC recommendations[1] with $\Xi(^{11}B) = 32.083974$ MHz and $\Xi(^{31}P) = 40.480742$ MHz. Additionally, compound **3** was studied by $^{31}P\{^{1}H\}$ HPdec/MAS NMR spectroscopy at 243.06 MHz using a Bruker Avance III HD 600 MHz NMR spectrometer. IR spectra were measured in the attenuated total reflection (ATR) mode in the region of 4000–530 cm^{-1} with an apodized resolution of 1 cm^{-1} with a Bruker Alpha spectrometer equipped with a Bruker diamond single reflection ATR system. Raman spectra were measured using the 1064 nm excitation line of a Nd/YAG laser on crystalline samples contained in melting point capillaries in the region of 3500–80 cm^{-1} at room temperature on a Bruker IFS-120 spectrometer with an apodized resolution of 1 cm^{-1}. ESI mass spectra were acquired on a microTOF (Bruker Daltonics). Elemental analysis (C, H, N) were performed either with a Euro EA3000 instrument (HEKA-Tech, Germany) or with an Elementar vario MICRO Cube elemental analyser.

Chemicals

All standard chemicals were obtained from commercial sources und used without further purification. Solvents were dried according to standard protocols[6] and stored in flasks equipped with valves with PTFE stems (Young, London) under an argon atmosphere. $[Ph_3PAuCl]$,[7] Cs[12-HC≡C-*closo*-1-$CB_{11}H_{11}$][8, 9] and {12-Ag_2C≡C-*closo*-1-$CB_{11}H_{11}$}$_n$[10] were prepared as described, elsewhere.

Syntheses

Synthesis of [Et$_4$N][12-(Ph$_3$PAu)C≡C-*closo*-1-CB$_{11}$H$_{11}$] ([Et$_4$N]1). $[Et_4N]$[12-HC≡C-*closo*-1-$CB_{11}H_{11}$] (48 mg, 0.16 mmol) was dissolved in ethanol (20 mL) and an aqueous solution of $[Et_4N]OH$ (0.5 mL, 20% w/w) was added. While stirring, a solution of $[Ph_3PAuCl]$ (82 mg, 0.16 mmol) in CH_2Cl_2 (3 mL) was added. The dichloromethane was removed under reduced pressure. The $[Et_4N]$**1** was filtered off, washed with ethanol (3 × 3 mL) and dried in a vacuum. Yield: 104 mg (0.14 mmol, 83%).

^{1}H{^{11}B} NMR (500.1 MHz, CD$_2$Cl$_2$, *δ*): 7.56–7.42 (m, 15H, Ph), 3.23 (q, 8H, $^{3}J(^{1}$H,^{1}H) = 7.45 Hz, CH$_2$, [Et$_4$N]$^+$), 2.18 (s, 1H, C$_{\text{cluster}}$–H), 1.61 (s, 10H, BH), 1.28 ppm (tt, 12H, $^{2}J(^{1}$H,^{1}H) = 1.85 Hz, $^{3}J(^{1}$H,^{1}H) = 7.45 Hz, CH$_3$, [Et$_4$N]$^+$).

^{13}C{^{1}H} NMR (125.8 MHz, CD$_2$Cl$_2$, *δ*): 138.4 (d br, 1C, $^{2}J(^{31}$P,^{13}C) ≈ 120 Hz, BC≡***C***), 134.6 (d, 6C, $J(^{31}$P,^{13}C) = 13.9 Hz, Ph), 131.9 (d, 3C, $J(^{31}$P,^{13}C) = 2.0 Hz, Ph), 130.7 (d, 3C, $J(^{31}$P,^{13}C) = 54.2 Hz, Ph), 129.5 (d, 6C, $J(^{31}$P,^{13}C) = 11.1 Hz, Ph), 116.6 (br, 1C, B***C***≡C), 53.1 (t, 4C, $^{1}J(^{14}$N,^{13}C) ≈ 2 Hz, CH$_2$, [Et$_4$N]$^+$), 47.8 (s, 1C, C$_{\text{cluster}}$), 8.0 ppm (s, 4C, CH$_3$, [Et$_4$N]$^+$).

^{11}B NMR (160.5 MHz, CD$_2$Cl$_2$, *δ*): −7.0 (s, 1B, B12), −12.2 (d, 5B, $^{1}J(^{11}$B,^{1}H) = 138 Hz, B7–11), −16.7 ppm (d, 5B, $^{1}J(^{11}$B,^{1}H) = 149 Hz, B2–6).

^{31}P{^{1}H} NMR (202.5 MHz, CD$_2$Cl$_2$, *δ*): 42.4 ppm (s, 1P, PPh$_3$).

^{11}B{^{1}H} RSHE/MAS NMR (128.4 MHz, δ_{iso}): −7.1 (s, 1B, B12), −12.3 (s, 5B, B7–11), −18.1 ppm (s, 5B, B2–6).

IR (ATR): $\tilde{\nu}$ = 2981 (w, *ν*(C–H)), 2590–2500 cm^{-1} (vs vbr, *ν*(B–H)).

Raman: $\tilde{\nu}$ = 3056 (s, *ν*(C–H)), 2986 (m, *ν*(C–H)), 2943 (m, *ν*(C–H)), 2590–2500 (s br, *ν*(B–H)), 2083 cm^{-1} (m, *ν*(C≡C)).

Elemental analysis calcd (%) for C$_{29}$H$_{46}$AuB$_{11}$NP: C, 46.10; H, 6.14; N, 1.85; found: C, 45.63; H, 6.17; N, 1.63.

Synthesis of [12-(Ph$_3$PAu)$_2$C≡C-*closo*-1-CB$_{11}$H$_{11}$] (2). Cs[12-HC≡C-*closo*-1-CB$_{11}$H$_{11}$] (70 mg, 0.23 mmol) was dissolved in ethanol (30 mL) and KOH was added (200 mg, 3.56 mmol). A solution of [Ph$_3$PAuCl] (231 mg, 0.47 mmol) in CH$_2$Cl$_2$ (5 mL) was added under stirring. The volume of the solution was reduced to approximately 15 mL with a rotary evaporator. Solid **2** that had formed was collected by filtration, washed with ethanol (2 × 5 mL) and dried in a vacuum. Yield: 244 mg (0.22 mmol, 96%).

^{1}H{^{11}B} NMR (500.1 MHz, CD$_2$Cl$_2$, *δ*): 7.53–7.33 (m, 30H, Ph), 2.32 (s, 1H, C$_{\text{cluster}}$–H), 1.83 (s, 5H, BH), 1.71 ppm (s, 5H, BH).

^{13}C{^{1}H} NMR (125.8 MHz, CD$_2$Cl$_2$, *δ*): 134.5 (d, 12C, $J(^{13}$C,^{31}P) = 14 Hz, Ph), 134.3 (qt, 1C, $^{1}J(^{13}$C,^{11}B) ≈ 90–100 Hz, $^{3}J(^{31}$P,^{13}C) ≈ 10 Hz, B***C***≡C), 132.4 (d, 6C, $J(^{13}$C,^{31}P) = 2.4 Hz, Ph), 132.4 (qt, 1C, $^{2}J(^{13}$C,^{11}B) ≈ 10–13 Hz, $^{2}J(^{31}$P,^{13}C) ≈ 70 Hz, BC≡***C***), 129.7 (d, 12C, $J(^{31}$P,^{13}C) = 12 Hz, Ph), 129.0 (d, 6C, $J(^{31}$P,^{13}C) = 60 Hz, Ph), 51.8 ppm (s, 1C, C$_{\text{Cluster}}$).

^{11}B NMR (160.5 MHz, CD$_2$Cl$_2$, *δ*): −9.4 (s, 1B, B12), −12.1 (d, 5B, $^{1}J(^{11}$B,^{1}H) = 140 Hz, B7–11), −16.1 ppm (d, 5B, $^{1}J(^{11}$B,^{1}H) = 153 Hz, B2–6).

^{31}P{^{1}H} NMR (202.5 MHz, CD$_2$Cl$_2$, *δ*): 36.0 ppm (s, 2P, PPh$_3$).

^{11}B{^{1}H} RSHE/MAS NMR (128.4 MHz, δ_{iso}): −9.1 (s, 1B, B12), −12.0 (s, 5B, B7–11), −15.8 ppm (s, 5B, B2–6).

IR (ATR): $\tilde{\nu}$ = 3054 (w, *ν*(C–H)), 2610–2400 cm^{-1} (s vbr, *ν*(B–H)).

Raman: $\tilde{\nu}$ = 3054 (vs, *ν*(C–H)), 2600–2460 (s br, *ν*(B–H)), 2004 cm^{-1} (s, *ν*(C≡C)).

Elemental analysis calcd (%) for $C_{39}H_{41}Au_2B_{11}P_2$: C**,** 43.19; H**,** 3.81; found: C, 42.91; H, 3.94.

Synthesis of [{12-(Ph$_3$PAg)$_2$C≡C-*closo*-1-CB$_{11}$H$_{11}$}$_2$] (3). {12-Ag$_2$C≡C-*closo*-1-CB$_{11}$H$_{11}$}$_n$ (80 mg, 0.21 mmol) was dissolved in a minimum amount of acetone. Triphenylphosphane (110 mg, 0.42 mmol) was added while stirring. The solution was cooled to 0 °C whereupon colorless crystals separated that were isolated by filtration, washed with three portions of hexane (3 × 5 mL) and dried in vacuum. Yield 160 mg (0.09 mmol, 84%).

^{1}H{^{11}B} NMR (500.1 MHz, (CD$_3$)$_2$SO, δ): 7.52–7.33 (m, 60H, Ph), 2.34 (s, 2H, C$_{\text{cluster}}$–H), 1.71 (s, 10H, BH), 1.55 ppm (s, 10H, BH).

^{13}C{^{1}H} NMR (125.8 MHz, (CD$_3$)$_2$SO, δ): 133.6 (d, 24C, J(^{13}C,^{31}P) = 16.3 Hz, Ph), 130.9 (d, 12C, J(^{13}C,^{31}P) = 30.4 Hz, Ph), 130.8 (d, 12C, J(^{13}C,^{31}P) = 1 Hz, Ph), 129.1 (d, 24C, J(^{31}P,^{13}C) = 9.9 Hz, Ph), 110.0 (vbr, 2C, BC≡C), 100.5 (vbr, 2C, BC≡C), 48.1 ppm (s, 2C, C$_{\text{Cluster}}$).

^{11}B NMR (160.5 MHz, (CD$_3$)$_2$SO, δ): −8.1 (s, 2B, B12), −12.1 (d, 10B, ^1J(^{11}B,^{1}H) = 135 Hz, B7–11), −16.6 ppm (d, 10B, ^1J(^{11}B,^{1}H) = 137 Hz, B2–6).

^{31}P{^{1}H} NMR (202.5 MHz, (CD$_3$)$_2$SO, δ): 10.1 ppm (s, 4P, PPh$_3$).

^{11}B{^{1}H} RSHE/MAS NMR (128.4 MHz, δ_{iso}): −8.4 (s, 1B, B12), −13.4 (s, 5B, B7–11), −18.1 ppm (s, 5B, B2–6).

IR (ATR): $\tilde{\nu}$ = 3054 (w, ν(C–H)) 2600–2440 cm^{-1} (s, ν(B–H)).

Raman: $\tilde{\nu}$ = 3056 (vs, ν(C–H)), 2605–2445 (vs, ν(B–H)), 2004 cm^{-1} (s, ν(C≡C)).

Elemental analysis calcd (%) for $C_{78}H_{82}Ag_4B_{22}P_4$: C**,** 51.68; H**,** 4.56; found: C, 51.71; H, 4.67.

Synthesis of [12-(Ph$_3$PAu){(Ph$_3$P)$_2$Ag}C≡C-*closo*-1-CB$_{11}$H$_{11}$] (4). [12-(Ph$_3$PAu)$_2$C≡C-*closo*-1-CB$_{11}$H$_{11}$] (**2**; 60 mg, 0.06 mmol) and PPh$_3$ (29 mg, 0.11 mmol) were dissolved in dimethyl sulfoxide (3 mL). A solution of {[12-(Ph$_3$PAg)$_2$C≡C-*closo*-1-CB$_{11}$H$_{11}$]}$_2$ (**3**; 50 mg, 0.03 mmol) in a minimum amount of dimethyl sulfoxide was added under stirring. The reaction mixture was stored without stirring. Crystalline **4** was isolated via filtration after 2 days. The solid was washed with three portions of benzene (3 × 3 mL) and dried in vacuum. Yield 86 mg (0.07 mmol, 62%).

^{1}H{^{11}B} NMR (500.1 MHz, CD$_2$Cl$_2$, δ): 7.43–7.20 (m, 45H, Ph), 2.20 (s, 1H, C$_{\text{cluster}}$–H), 1.70 (s, 5H, BH), 1.58 ppm (s, 5H, BH).

^{13}C{^{1}H} NMR (125.8 MHz, CD$_2$Cl$_2$, δ): 134.4 (d, 18C, J(^{13}C,^{31}P) = 15 Hz, Ph), 131.5–131.0 (vbr, 9C, Ph), 131.2 (s, 9C, Ph), 129.4 (d, 18C, J(^{13}C,^{31}P) = 10 Hz, Ph), 126.1 (br, 1C, B***C***≡C), 119.5 (q br, 1C, ^1J(^{13}C,^{11}B) ≈ 95 Hz, B***C***≡C), 49.7 ppm (s, 1C, C$_{\text{Cluster}}$).

^{11}B NMR (160.5 MHz, CD$_2$Cl$_2$, δ): −8.7 (s, 1B, B12), −12.2 (d, 5B, ^1J(^{11}B,^{1}H) = 139 Hz, B7–11), −16.4 ppm (d, 5B, ^1J(^{11}B,^{1}H) = 150 Hz, B2–6).

^{31}P{^{1}H} NMR (202.5 MHz, CD$_2$Cl$_2$, δ): 38.5 (s vbr, 1P, AuPPh$_3$), 7.9 ppm (s vbr, 2P, AgPPh$_3$).

$^{11}B\{^1H\}$ RSHE/MAS NMR (128.4 MHz, δ_{iso}): −7.9/−8.3 (1B, B12), −12.0 (s, 5B, B7−11), −15.4 ppm (s, 5B, B2−6).

IR (ATR): $\tilde{\nu}$ = 3052 (m, ν(C–H)), 2600–2340 cm^{-1} (vs, ν(B–H)).

Raman: $\tilde{\nu}$ = 3053 (vs, ν(C–H)), 2610–2490 (m, ν(B–H)), 2042 cm^{-1} (m, ν(C≡C)).

Elemental analysis calcd (%) for $C_{57}H_{56}AgAuB_{11}P_3$: C**,** 54.43; H**,** 4.49; found: C, 54.06; H, 4.75.

Crystal Structure Determination

Colourless crystals of $[Et_4N][12\text{-}(Ph_3PAu)C{\equiv}C\text{-}$*closo*$\text{-}1\text{-}CB_{11}H_{11}]\cdot 2THF$ ($[Et_4N]$**1**$\cdot$2THF) were obtained from dichloromethane/THF by slow evaporation of the solvents. $[12\text{-}(Ph_3PAu)_2C{\equiv}C\text{-}$*closo*$\text{-}1\text{-}CB_{11}H_{11}]$ (**2**) was crystallized from diethyl ether, acetone and dichloromethane to give colourless crystals of **2**$\cdot Et_2O$, **2**$\cdot(CH_3)_2CO$ and **2**$\cdot CH_2Cl_2$, respectively. Similarly, colourless crystals of $[\{12\text{-}(Ph_3PAg)_2C{\equiv}C\text{-}$*closo*$\text{-}1\text{-}CB_{11}H_{11}\}_2]\cdot 2(CH_3)_2SO$ (**3**$\cdot 2(CH_3)_2SO$), $[\{12\text{-}(Ph_3PAg)_2C{\equiv}C\text{-}$*closo*$\text{-}1\text{-}CB_{11}H_{11}\}_2]\cdot 2CH_3CN$ (**3**$\cdot 2CH_3CN$) and $[\{12\text{-}(Ph_3PAg)_2C{\equiv}C\text{-}$*closo*$\text{-}1\text{-}CB_{11}H_{11}\}_2]\cdot C_6H_6\cdot CH_3CN$ (**3**$\cdot C_6H_6\cdot CH_3CN$) were obtained from dimethyl sulfoxide (DMSO), acetonitrile and a mixed solvent system of benzene and acetonitrile. Single crystals of colourless $[12\text{-}(Ph_3PAu)\{(Ph_3P)_2Ag\}C{\equiv}C\text{-}$*closo*$\text{-}1\text{-}CB_{11}H_{11}]$ (**4**) were obtained from a DMSO solution. Crystals were investigated either with a Bruker X8-Apex II diffractometer ($[Et_4N]$**1**$\cdot$2THF, **2**$\cdot CH_2Cl_2$, **3**$\cdot 2(CH_3)_2SO$, **3**$\cdot 2CH_3CN$, **3**$\cdot C_6H_6\cdot CH_3CN$, **4**), a Stoe STADI CCD diffractometer (**2**$\cdot(CH_3)_2CO$) or a Oxford Xcalibur diffractometer (**2**$\cdot Et_2O$) using Mo-Kα radiation (λ = 0.71073 Å) in all cases. All structures were solved either by direct (SHELXS)[11, 12] or by intrinsic phasing methods (SHELXT).[11, 13] Refinements are based on full-matrix least-squares calculations on F^2.[11, 14] The tetraethylammonium cations and one of the two crystallographically independent THF molecules in the crystal of $[Et_4N]$**1**$\cdot$2THF are strongly disordered. So, their contributions to the structure factors were secured by back-Fourier transformation using the SQUEEZE routine as of the program PLATON, resulting in 886 electrons per unit cell.[15-17] All non-hydrogen atoms were refined anisotropically. The positions of most of the H atoms were located from electron density difference maps. In the final steps of the refinement idealized bond lengths and angles were introduced. Calculations were performed with the ShelXle graphical interface.[18] Molecular structure diagrams were drawn with the program Diamond 4.5.2.[19] Experimental details, crystal data, and the CCDC numbers are collected in Table S1. These data can be obtained free of charge from The Cambridge Crystallographic Data Centre via www.ccdc.cam.ac.uk/data_request/cif.

Table S1. Selected Crystal Data and Details of the Refinement of the Crystal Structures of [$\mathrm{Et_4N}$][12-($\mathrm{Ph_3PAu}$)C≡C-*closo*-1-$\mathrm{CB_{11}H_{11}}$]·2THF ([$\mathrm{Et_4N}$]**1**·2THF), [12-($\mathrm{Ph_3PAu}$)$_2$C≡C-*closo*-1-$\mathrm{CB_{11}H_{11}}$]·$\mathrm{Et_2O}$ (**2**·$\mathrm{Et_2O}$), [12-($\mathrm{Ph_3PAu}$)$_2$C≡C-*closo*-1-$\mathrm{CB_{11}H_{11}}$]·$\mathrm{(CH_3)_2CO}$ (**2**·$\mathrm{(CH_3)_2CO}$), [12-($\mathrm{Ph_3PAu}$)$_2$C≡C-*closo*-1-$\mathrm{CB_{11}H_{11}}$]·$\mathrm{CH_2Cl_2}$ (**2**·$\mathrm{CH_2Cl_2}$), [{12-($\mathrm{Ph_3PAg}$)$_2$C≡C-*closo*-1-$\mathrm{CB_{11}H_{11}}$}$_2$]·2$\mathrm{(CH_3)_2SO}$ (**3**·2$\mathrm{(CH_3)_2SO}$), [{12-($\mathrm{Ph_3PAg}$)$_2$C≡C-*closo*-1-$\mathrm{CB_{11}H_{11}}$}$_2$]·2$\mathrm{CH_3CN}$ (**3**·2$\mathrm{CH_3CN}$), [{12-($\mathrm{Ph_3PAg}$)$_2$C≡C-*closo*-1-$\mathrm{CB_{11}H_{11}}$}$_2$]·$\mathrm{C_6H_6}$·$\mathrm{CH_3CN}$ (**3**·$\mathrm{C_6H_6}$·$\mathrm{CH_3CN}$) and [12-($\mathrm{Ph_3PAu}$){($\mathrm{Ph_3P}$)$_2$Ag}C≡C-*closo*-1-$\mathrm{CB_{11}H_{11}}$] (**4**).

	[$\mathrm{Et_4N}$]**1**·2THF[a]	**2**·$\mathrm{Et_2O}$	**2**·$\mathrm{(CH_3)_2CO}$	**2**·$\mathrm{CH_2Cl_2}$	**3**·2$\mathrm{(CH_3)_2SO}$	**3**·2$\mathrm{CH_3CN}$	**3**·$\mathrm{C_6H_6}$·$\mathrm{CH_3CN}$	**4**
Formula	$\mathrm{C_{46}H_{60}Au_2B_{22}OP_2}$	$\mathrm{C_{43}H_{51}Au_2B_{11}OP_2}$	$\mathrm{C_{42}H_{47}Au_2B_{11}OP_2}$	$\mathrm{C_{40}H_{43}Au_2B_{11}Cl_2P_2}$	$\mathrm{C_{82}H_{94}Ag_4B_{22}O_2P_4S_4}$	$\mathrm{C_{86}H_{94}Ag_4B_{22}N_4P_4}$	$\mathrm{C_{86}H_{91}Ag_4B_{22}NP_4}$	$\mathrm{C_{57}H_{56}AgAuB_{11}P_3}$
M_W	1322.63	1158.62	1142.58	1169.42	1968.87	1976.83	1931.77	1257.67
T (K)	100(2)	273(2)	290(2)	100(2)	100(2)	100(2)	100(2)	100(2)
Crystal system	monoclinic	triclinic	triclinic	triclinic	monoclinic	monoclinic	triclinic	orthorhombic
Space group	$P2_1/c$	P–1	P–1	P–1	$P2_1/n$	$P2_1/n$	P–1	$Pca2_1$
a (Å)	32.353(2)	12.4449(4)	11.145(2)	11.2596(5)	13.4734(9)	13.5094(5)	13.7720(5)	20.5131(16)
b (Å)	9.0652(5)	14.1794(5)	12.322(3)	12.2332(6)	16.7754(12)	16.2013(7)	14.7348(5)	21.0277(17)
c (Å)	26.6939(16)	14.3583(5)	18.366(4)	18.0030(9)	19.1508(13)	20.8836(8)	23.9233(9)	25.367(2)
α		83.949(3)	84.17(3)	80.9350(10)			83.4210(10)	
β	113.503(3)	85.674(3)	76.36(3)	75.0080(10)	91.565(2)	91.9370(10)	76.8810(10)	
γ		73.294(3)	68.33(3)	68.4270(10)			67.2960(10)	
volume (Å^3)	77179.6(8)	2410.51(15)	2277.5(10)	2222.16(19)	4326.9(5)	4568.2(3)	4359.7(3)	10941.8(15)
Z	4	2	2	2	2	2	2	8
d(calcd) (Mg m^{-3})	1.224	1.596	1.666	1.748	1.511	1.437	1.472	1.527
μ (mm^{-1})	4.154	6.177	6.537	6.816	1.061	0.961	1.004	3.162
F(000)	2568	1120	1100	1120	1984	1992	1944	4992
No. of collected reflections	58236	16920	20181	22520	60612	29492	60774	123726
No. of unique reflections	15298	9476	7914	9457	9412	8955	18621	22489
R(int)	0.0428	0.0351	0.0550	0.0173	0.0365	0.0249	0.0266	0.0503
No. of parameters / restraints	566 / 12	534 / 36	524 / 0	514 / 0	569 / 0	543 / 0	1055 / 0	1316 / 1
$R1$ ($I > 2\sigma(I)$)	0.0929	0.0481	0.0546	0.0170	0.0225	0.0235	0.0319	0.0271
$wR2$ (all)	0.1949	0.1402	0.1610	0.0406	0.0505	0.0579	0.0819	0.0566
GOF on F^2	3.810	1.020	1.033	1.029	1.036	1.085	1.027	1.023
Largest diff. peak / hole / e Å^{-3}	10.268 / –7.981	3.380 / –1.627	3.098 / –2.929	1.333 / –0.569	0.409 / –0.342	0.432 / –0.298	0.961 / –1.047	1.225 / –0.962
CCDC no.	1856194	1856195	1856196	1856197	1856198	1856199	1856200	1856201

[a] The [$\mathrm{Et_4N}$]$^+$ ions and one of the two THF molecules are strongly disordered. Thus, their contributions to the structure factors were secured by back-Fourier transformation using the SQUEEZE routine.

Table S2. Selected Interatomic Distances and Angles of [Et$_4$N][12-(Ph$_3$PAu)C≡C-*closo*-1-CB$_{11}$H$_{11}$]·2THF ([Et$_4$N]**1**·2THF), [12-(Ph$_3$PAu)$_2$C≡C-*closo*-1-CB$_{11}$H$_{11}$]·Et$_2$O (**2**·Et$_2$O), [12-(Ph$_3$PAu)$_2$C≡C-*closo*-1-CB$_{11}$H$_{11}$]·(CH$_3$)$_2$CO (**2**·(CH$_3$)$_2$CO), [12-(Ph$_3$PAu)$_2$C≡C-*closo*-1-CB$_{11}$H$_{11}$]·CH$_2$Cl$_2$ (**2**·CH$_2$Cl$_2$), [{12-(Ph$_3$PAg)$_2$C≡C-*closo*-1-CB$_{11}$H$_{11}$}$_2$]·2(CH$_3$)$_2$SO (**3**·2(CH$_3$)$_2$SO), [{12-(Ph$_3$PAg)$_2$C≡C-*closo*-1-CB$_{11}$H$_{11}$}$_2$]·2CH$_3$CN (**3**·2CH$_3$CN), [{12-(Ph$_3$PAg)$_2$C≡C-*closo*-1-CB$_{11}$H$_{11}$}$_2$]·C$_6$H$_6$·CH$_3$CN (**3**·C$_6$H$_6$·CH$_3$CN) and [12-(Ph$_3$PAu){(Ph$_3$P)$_2$Ag}C≡C-*closo*-1-CB$_{11}$H$_{11}$] (**4**).

	[Et$_4$N]**1**·2THF		**2**·Et$_2$O	**2**·(CH$_3$)$_2$CO	**2**·CH$_2$Cl$_2$	**3**·2(CH$_3$)$_2$SO	**3**·2CH$_3$CN	**3**·C$_6$H$_6$·CH$_3$CN		**4**	
	#1[a]	#2[a]						#1[a]	#2[a]	#1[a]	#2[a]
d(C≡C)	123.3(17)	118.1(17)	124.3(13)	126.0(11)	122.5(3)	121.9(3)	122.0(3)	122.5(3)	122.6(5)	122.7(10)	121.5(10)
d(B–C)	151.8(17)	156.6(17)	153.2(14)	154.3(12)	155.1(4)	154.7(3)	155.3(3)	155.9(4)	155.7(5)	153.7(11)	155.5(10)
d(C–M$_\sigma$)	200.4(11)	199.7(12)	200.8(9)	198.4(9)	201.2(2)	209.08(19)	208.43(19)	208.7(2)	208.7(3)	198.9(7)	199.7(7)
d(BC···M$_\pi$)	–	–	231.0(8)	234.9(8)	234.6(2)	273.43(18) 263.70(17)	280.37(19) 252.26(18)	272.0(3) 252.9(3)	274.4(3) 258.7(3)	252.8(7)	249.9(7)
d(M$_\sigma$C···M$_\pi$)	–	–	221.1(9)	215.8(9)	218.8(2)	253.60(18) 227.47(18)	248.4(2) 235.63(19)	255.5(3) 237.8(3)	246.6(3) 235.5(2)	238.8(6)	240.3(6)
d(M$_\sigma$–P)	228.3(3)	227.9(3)	226.4(3)	225.6(2)	226.85(7)	237.94(6)	237.74(6)	237.67(8)	237.70(8)	227.09(18)	228.01(18)
d(M$_\pi$–P)	–	–	224.1(2)	223.9(2)	224.81(6)	237.57(6)	239.41(6)	240.44(7)	239.25(7)	246.23(18) 245.04(18)	245.0(18) 247.8(18)
d(M$_\sigma$···M$_\pi$)	–	–	322.18(5)	310.26(9)	310.25(5)	328.52(6) 378.96(5)	333.35(6) 374.47(6)	358.84(7) 375.10(4)	354.21(5) 362.58(5)	332.30(6)	337.17(6)
d(M$_\pi$···M$_\pi$)	–	–	–	–	–	323.68(5)	338.00(5)	343.44(5)	320.38(3)	–	–
∡(B–C≡C)	176.4(14)	175.9(14)	174.1(9)	173.7(8)	172.0(2)	179.37(19)	174.95(19)	177.1(3)	176.5(3)	177.2(7)	177.3(7)
∡(C≡C–M$_\sigma$)	177.7(12)	172.1(12)	175.5(8)	176.1(7)	176.4(2)	161.93(16)	161.29(16)	162.6(2)	161.4(2)	170.7(6)	170.7(6)
∡(C–M$_\sigma$–P)	178.5(4)	176.3(4)	175.7(3)	177.3(3)	177.33(7)	158.97(6)	163.97(6)	160.42(8)	163.31(8)	173.9(2)	174.2(2)

[a] Two independent formula units.

Diffusion-Ordered Spectroscopy (DOSY)

^{1}H DOSY measurements were performed at 20 °C in 5 mm NMR tubes on a Bruker Avance III HD 600 spectrometer equipped with a 5 mm BBFH probe (^{1}H/X with $X = {}^{15}$N–^{31}P and ^{19}F) with z axis gradient coil capable of producing pulsed magnetic field gradients of 50 G/cm. Samples were studied as dilute solutions in $(CD_3)_2SO$. Temperature calibration was performed with standard samples of 0.2% CH_3OH in CD_3OD and 80% ethylene glycol in $(CD_3)_2SO$. Data were acquired and processed using the Bruker software Topspin 3.2. The DOSY data were recorded with the stimulated echo BPP-LED pulse sequence[20] (longitudinal eddy current delay sequence with bipolar gradient pulse pairs for diffusion and additional spoil gradients after the second and fourth 90° pulse). The diffusion time Δ was kept constant in each DOSY experiment while the 'smoothed square' diffusion gradients were incremented from 2 to 98% of maximum gradient strength in 32 linear steps. No ^{11}B decoupling was used to avoid heating of the sample. One component fittings of the gradient strength dependence of the signal intensities were performed by a Levenberg-Marquardt algorithm incorporated in the Bruker software Topspin 3.2. The experimental intensities show no systematic and only very small random deviations from a Gaussian decay curve.

The Stokes-Einstein equation[21-23] modified for the size of the diffusion molecule[24, 25] was used for the calculation of the pseudo-spherical hydrodynamic radii (r_h):

$$D_\mathrm{t} = \frac{k_\mathrm{B}T\left(1 + 0.695\left(\frac{r_\mathrm{solv}}{r_\mathrm{h}}\right)^{2.234}\right)}{6\pi\eta r_\mathrm{h}} = \text{diffusion constant}$$

$T = \text{absolute temperature}$

$k_\mathrm{B} = \text{Boltzmann constant}$

$\eta((\mathrm{CD_3})_2\mathrm{SO}, 25\,°\mathrm{C}) = 2.170 \cdot 10^{-4}\ \text{mPa s} = \text{fluid viscosity (calculated from } D_\mathrm{t}(\mathrm{TMSS})_\mathrm{solv})$

$r_\mathrm{solv} = r_\mathrm{vdW}((\mathrm{CD_3})_2\mathrm{SO}) = 272\ \mathrm{pm}^{26}$

In Table S3 the hydrodynamic radii are compared to radii derived from single-crystal X-ray diffraction studies for [12-HC≡C-*closo*-1-$CB_{11}H_{11}]^-$ and **2**–**4**. V_molecule was calculated from the unit cell volume and Z. The radii were calculated assuming spherical coinage metal(I) complexes. For the calculation of the radii of the monomer of **3**, one monomer of the dimer was removed from the crystallographic files and the free volume was calculated using the VOID instruction of the PLATON program package.[16] Similarly, contributions of solvate molecules were removed from the cell volume to assess V_molecule.

Table S3. Comparison of the hydrodynamic radii of **2**–**4** and [12-HC≡C-*closo*-1-$CB_{11}H_{11}$]$^{-}$ in $(CD_3)_2SO$ calculated from the diffusion constants derived from the data of the H atoms bonded to the {*closo*-1-CB_{11}} cage ($H_{cluster}$) and those of the phenyl rings (H_{phenyl}) at 25 °C (r_h) to radii derived from crystal structure data (*vide supra*).

Compound	[12-HC≡C-*closo*-1-$CB_{11}H_{11}$]$^{-}$	**2**	**3**	**4**
D ($H_{cluster}$) [10^{-10} m^2 s^{-1}]	3.2425	1.6212	1.6212	1.6327
D (H_{phenyl}) [10^{-10} m^2 s^{-1}]	–	1.6072	1.5989	1.7606
r_h ($H_{cluster}$) [pm]	401	677	677	673
r_h (H_{phenyl}) [pm]	–	682	685	632
structure	Cs[12-HC≡C-*closo*-1-$CB_{11}H_{11}$][9]	**2**·CH_2Cl_2	**3**·2CH_3CN	**4**
$r_{monomer}$ (crystal) [pm]	356	613	579[a]	685
r_{dimer} (crystal) [pm]	–	–	769	–
$r_h/r_{monomer}$ ($H_{cluster}$)	0.89	0.90	1.14	1.02
r_h/r_{dimer} ($H_{cluster}$)	–	–	0.86	–
$r_h/r_{monomer}$ (H_{phenyl})	–	0.89	1.12	1.08
r_h/r_{dimer} (H_{phenyl})	–	–	0.85	–

[a] Extrapolated from $r_{monomer}$ of **1**, **2**, and **3**.

Photophysical measurements. Excitation and emission spectra were recorded on an Edinburgh Instrument FLSP920 spectrometer, equipped with a 450 W Xenon arc lamp, double monochromators for the excitation and emission pathways, and a red-sensitive photomultiplier (PMT-R928) as detector. The excitation and emission spectra were corrected using the standard corrections supplied by the manufacturer for the spectral power of the excitation source and the sensitivity of the detector. The quantum yields were measured by use of an integrating sphere with an Edinburgh Instrument FLSP920 spectrometer. The luminescence lifetimes were measured either using a µF920 pulsed 60 W Xenon microsecond flashlamp, with a repetition rate of 10-100 Hz, and a multichannel scaling module, or with a TCSPC module operating with pulsed laser diodes (pulse width ca. 200 ps, instrument response function ca. 800 ps). The emission was collected at right angles to the excitation source with the emission wavelength selected using a double grated monochromator and detected by the PMT. Low temperature measurements were conducted with an Optistat cryostate.

Cyclic Voltammetry Experiments. Cyclic voltammetry experiments were performed with a Metrohm PGSTAT30 potentiostat. Compounds [Et_4N]**1**, **2**–**4** and [Et_4N][12-HC≡C-*closo*-1-$CB_{11}H_{11}$] were dissolved in 3 mL acetonitrile that contained 0.1 mol L^{-1} [$n$$Bu_4N$][$PF_6$]. A standard three-electrode cell configuration was employed with a Pt working electrode (Ø = 3 mm), a Pt wire counter electrode, and an Ag/$AgNO_3$ reference electrode (0.01 mol L^{-1} $AgNO_3$ in acetonitrile that contained 0.1 mol L^{-1} [$n$$Bu_4N$][$PF_6$]), separated by a Vycor tip.

Computational Details. Calculations (gas-phase) were performed with the ORCA 4.0.1 program suite[27] using the PBE0[28-34] functional as implemented in ORCA together with the def2-SVP[35, 36] basis set for all atoms, and the respective ECP for the metal atoms, and the auxiliary basis set def2-SVP/J in order to accelerate the computations within the framework of RI approximation. Single point energy and orbital calculations were carried out by using the geometries available from our single crystal X-ray diffraction experiments. Van der Waals interactions have been considered by an empirical dispersion correction (Grimme-D3BJ).[37, 38] TD-DFT calculations for the first 20 vertical (Franck-Condon) singlet and triplet excited states were performed with the same functional and basis sets. Representations of molecular orbitals were produced with orca_plot as provided by ORCA 4.0.1 and with gOpenMol 3.00.[39, 40]

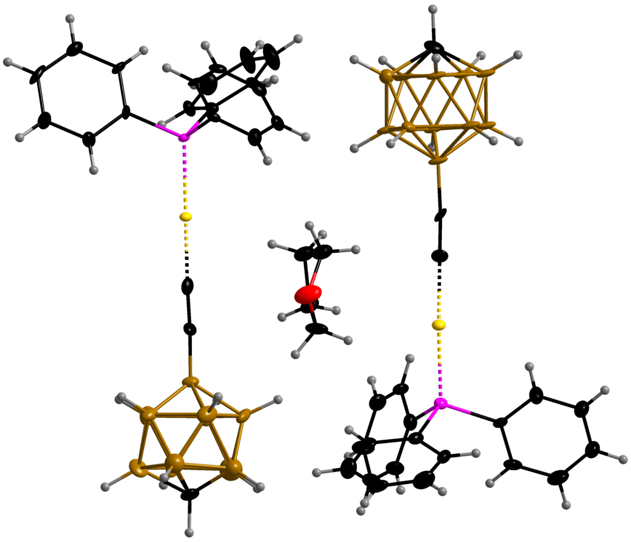

Figure S1. Both independent [12-(Ph$_3$PAu)C≡C-*closo*-1-CB$_{11}$H$_{11}$]$^-$ ions (**1**) and one of the two independent THF molecules in the crystal of [Et$_4$N]**1**·2THF. The second THF molecule and both crystallographically independent [Et$_4$N]$^+$ cations are strongly disordered. Therefore, their contributions to the structure factors were secured by back-Fourier transformation using the SQUEEZE routine as of the program PLATON, resulting in 886 electrons per unit cell.[15-17] Displacement ellipsoids are shown at 50% probability. The H atoms are depicted with arbitrary radii.

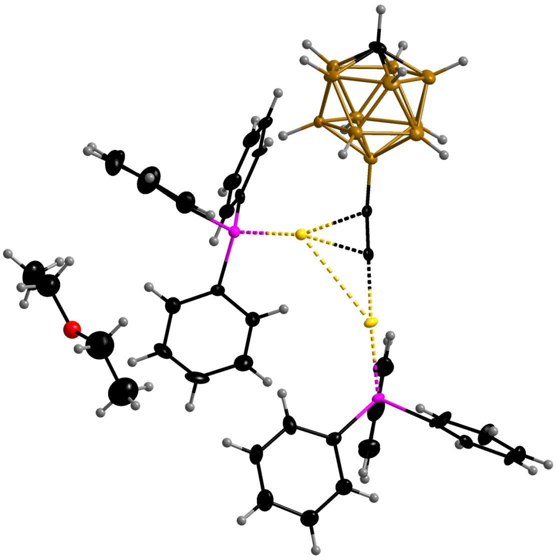

Figure S2. One formula unit of [12-$(Ph_3PAu)_2C{\equiv}C$-*closo*-1-$CB_{11}H_{11}$]·Et_2O (**2**·Et_2O) in the crystal. Displacement ellipsoids are shown at 30% probability. The H atoms are depicted with arbitrary radii.

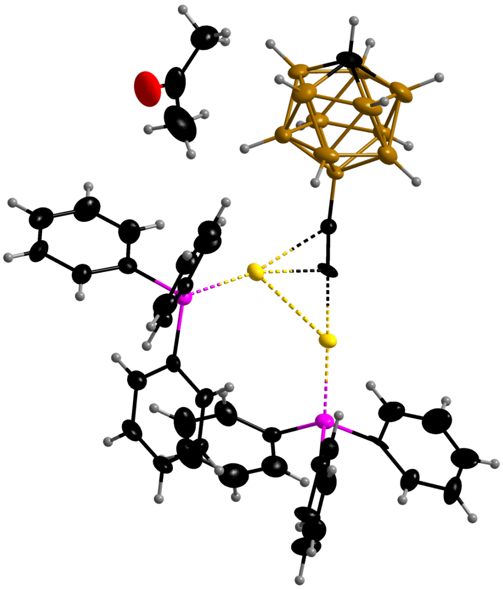

Figure S3. One formula unit of [12-$(Ph_3PAu)_2C{\equiv}C$-*closo*-1-$CB_{11}H_{11}$]·$(CH_3)_2CO$ (**2**·$(CH_3)_2CO$) in the crystal. Displacement ellipsoids are shown at 30% probability. The H atoms are depicted with arbitrary radii.

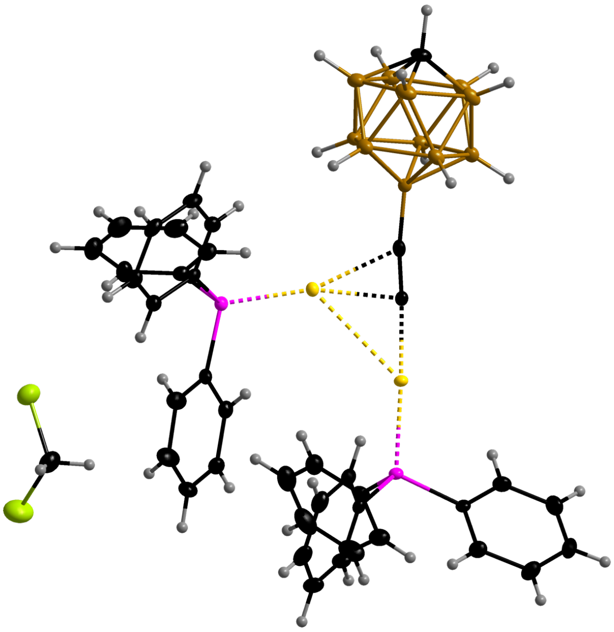

Figure S4. One formula unit of [12-$(Ph_3PAu)_2C{\equiv}C$-*closo*-1-$CB_{11}H_{11}$]·CH_2Cl_2 (**2**·CH_2Cl_2) in the crystal. Displacement ellipsoids are shown at 50% probability. The H atoms are depicted with arbitrary radii.

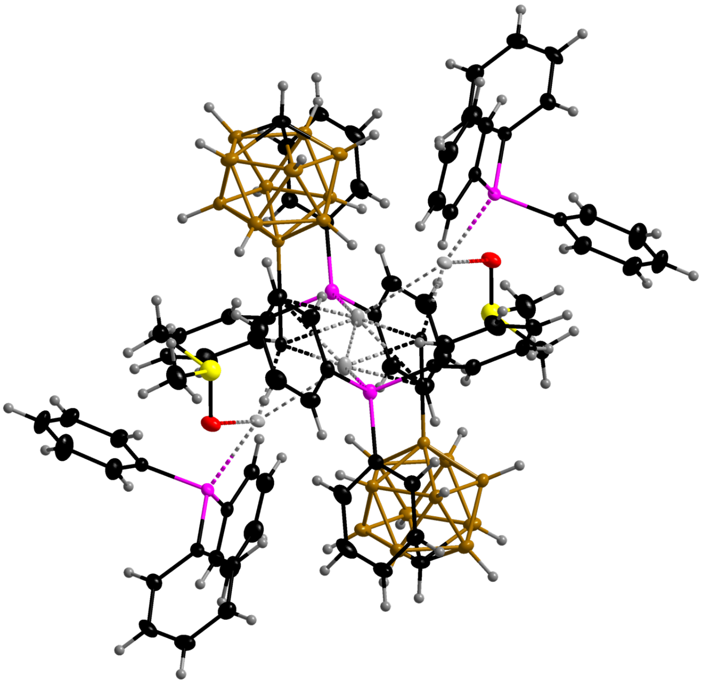

Figure S5. One formula unit of [{12-$(Ph_3PAg)_2C{\equiv}C$-*closo*-1-$CB_{11}H_{11}$}$_2$]·2$(CH_3)_2SO$ (**3**·2$(CH_3)_2SO$) in the crystal. Displacement ellipsoids are shown at 50% probability. The H atoms are depicted with arbitrary radii.

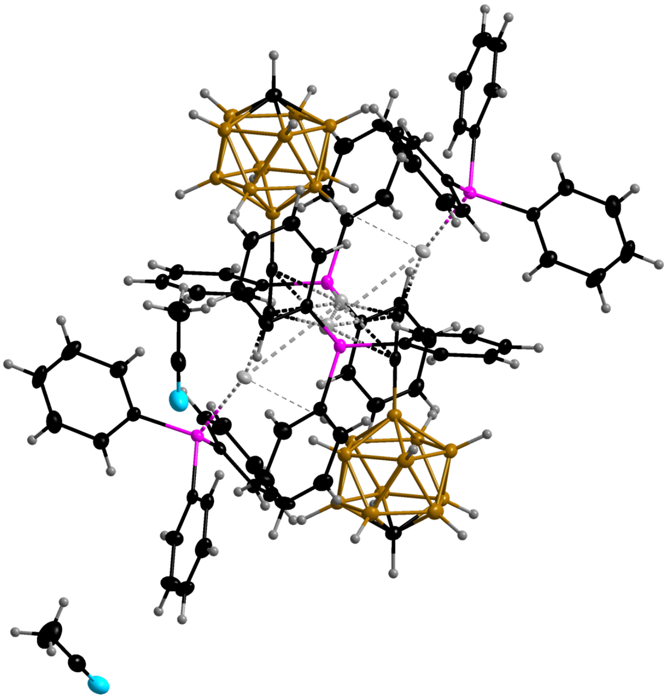

Figure S6. One formula unit of [{12-(Ph_3PAg)$_2$C≡C-*closo*-1-$CB_{11}H_{11}$}$_2$]·2CH_3CN (**3**·2CH_3CN) in the crystal. Displacement ellipsoids are shown at 50% probability. The H atoms are depicted with arbitrary radii.

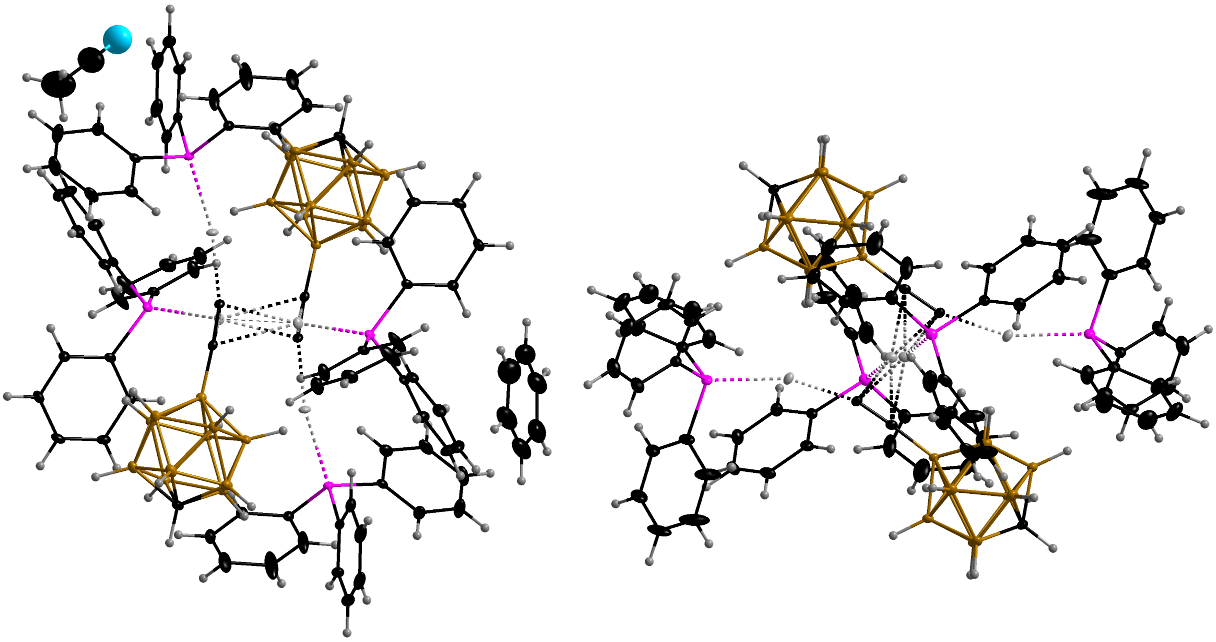

Figure S7. Both independent formula units of the complex [{12-(Ph_3PAg)$_2$C≡C-*closo*-1-$CB_{11}H_{11}$}$_2$] that are both located on a centre of inversion and one formula unit of C_6H_6 and CH_3CN in the crystal of **3**·C_6H_6·CH_3CN. Displacement ellipsoids are shown at 50% probability. The H atoms are depicted with arbitrary radii.

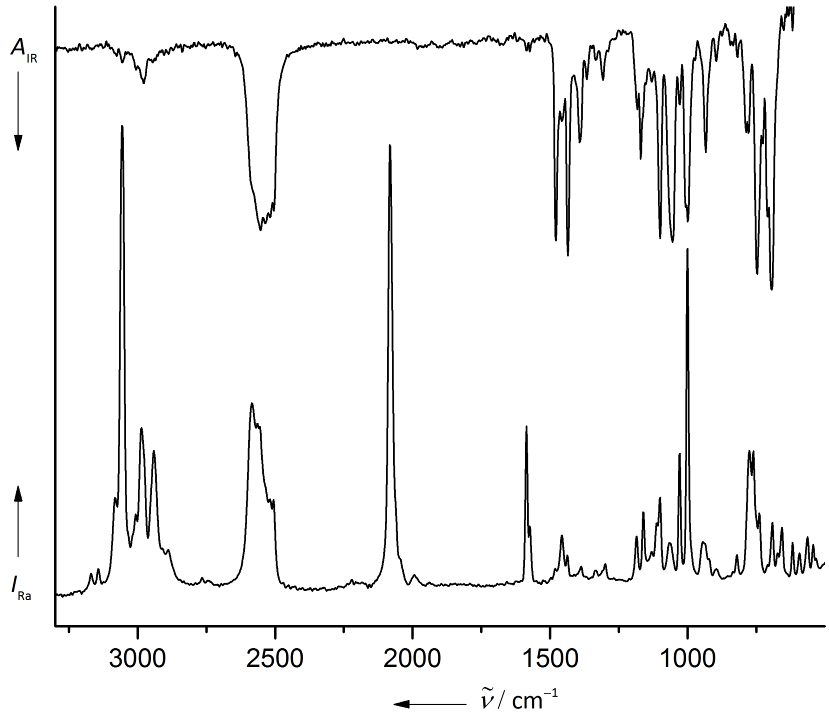

Figure S8. IR and Raman spectrum of [Et$_4$N]**1**.

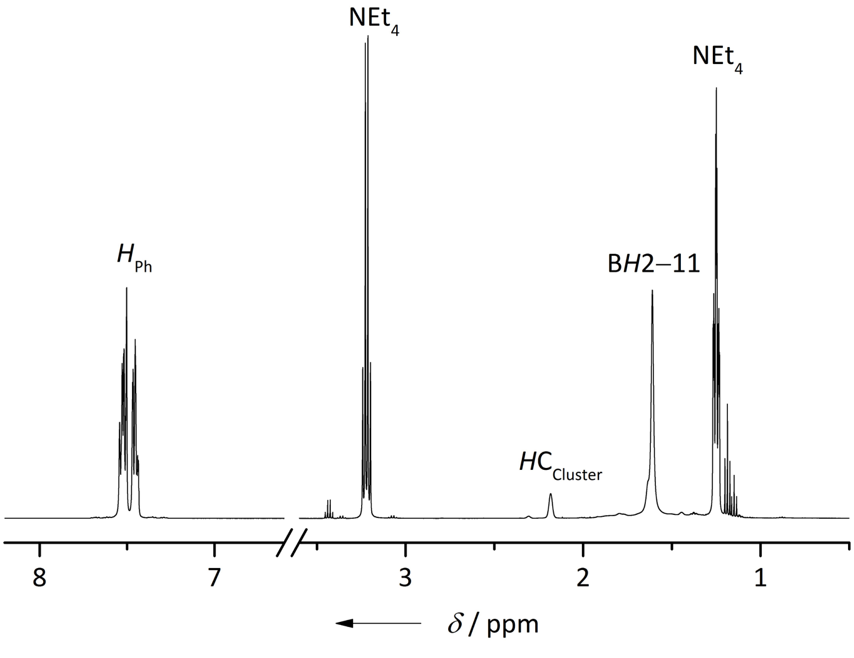

Figure S9. ^{1}H{^{11}B} NMR spectrum of [Et$_4$N]**1**.

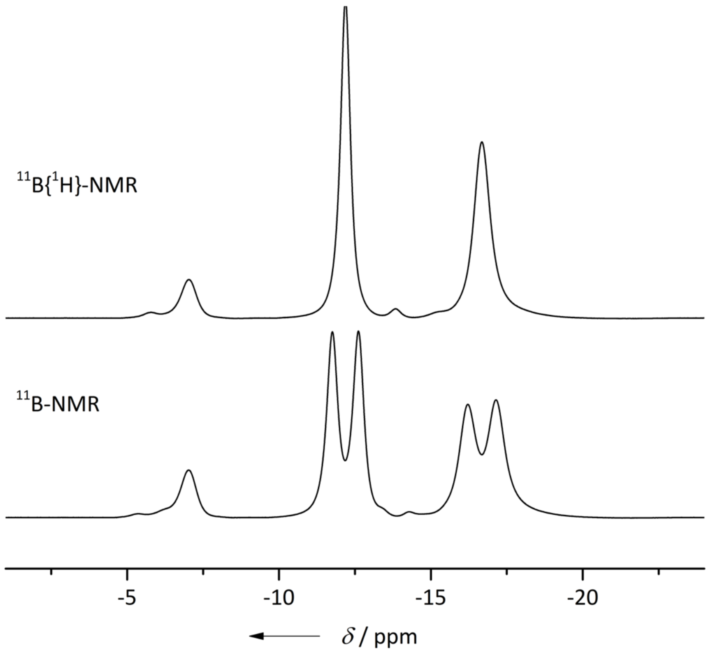

Figure S10. ^{11}B and $^{11}B\{^{1}H\}$ NMR spectra of [Et$_4$N]**1**.

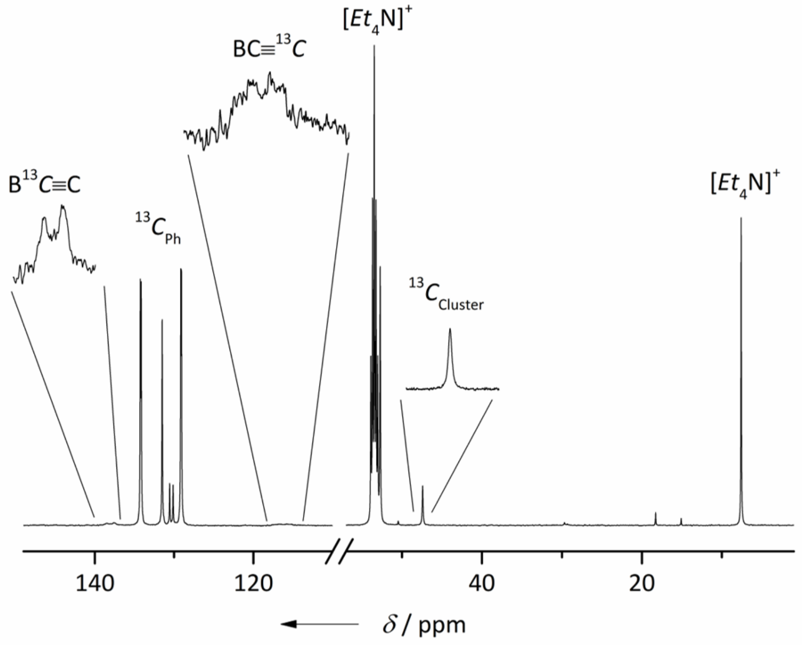

Figure S11. $^{13}C\{^{1}H\}$ NMR spectra of [Et$_4$N]**1**.

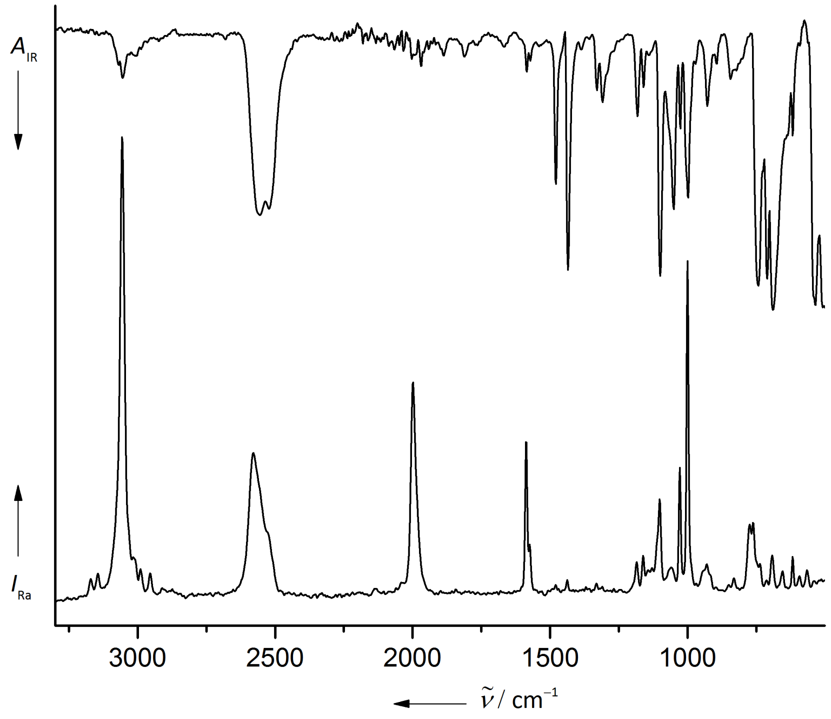

Figure S12. IR and Raman spectrum of **2**.

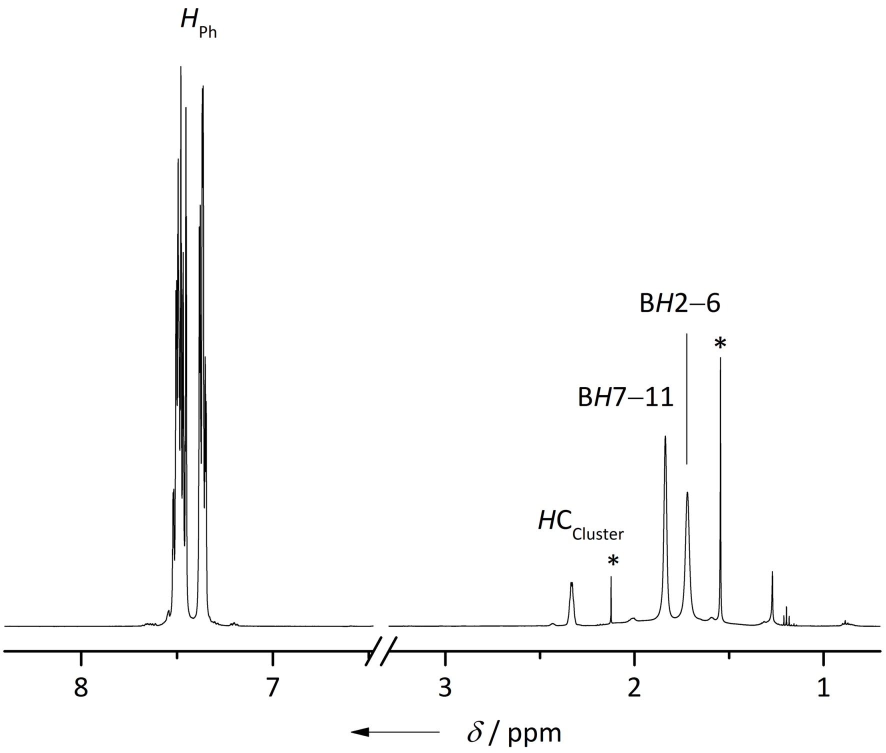

Figure S13. ^{1}H{^{11}B} NMR spectrum of **2**.

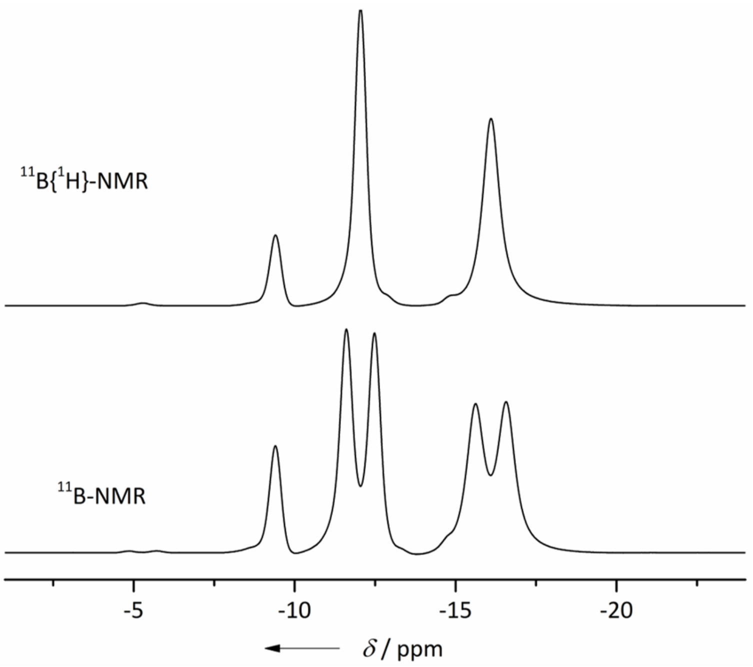

Figure S14. ^{11}B and ^{11}B{^{1}H} NMR spectra of **2**.

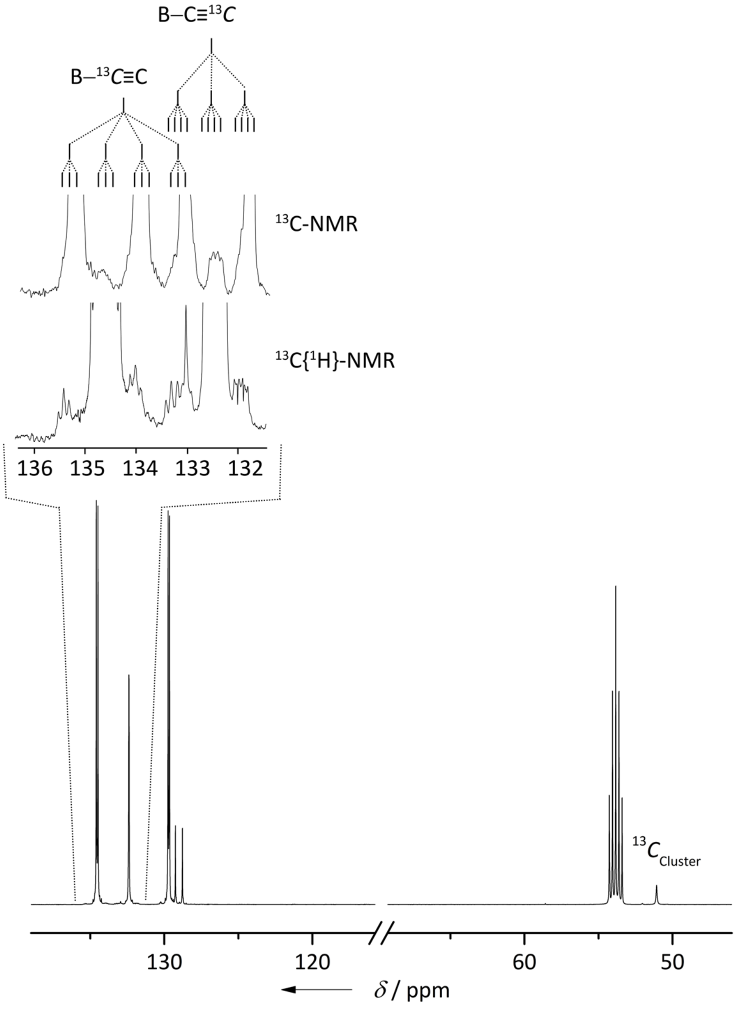

Figure S15. ^{13}C{^{1}H} NMR spectra of **2**.

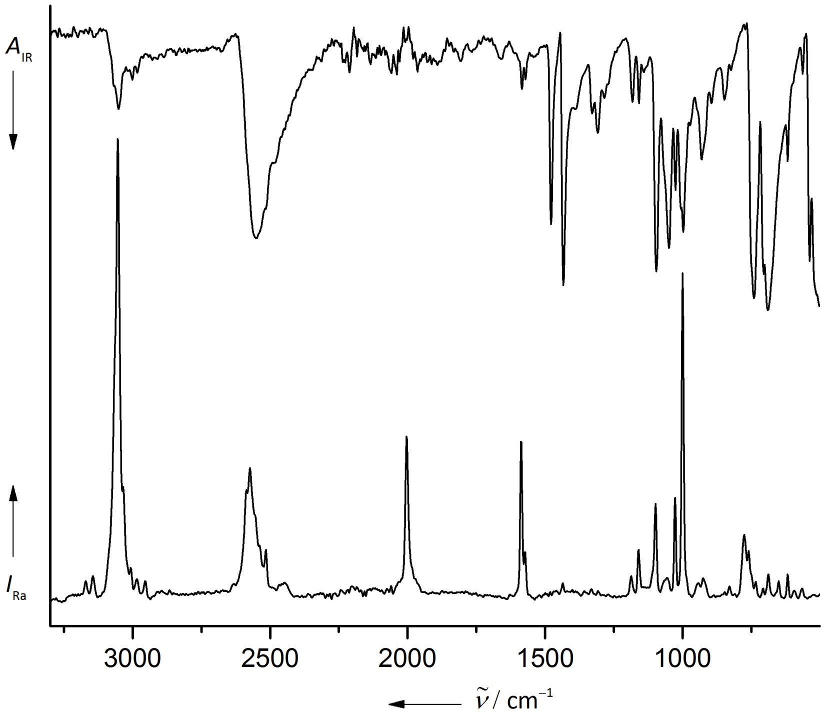

Figure S16. IR and Raman spectrum of **3**.

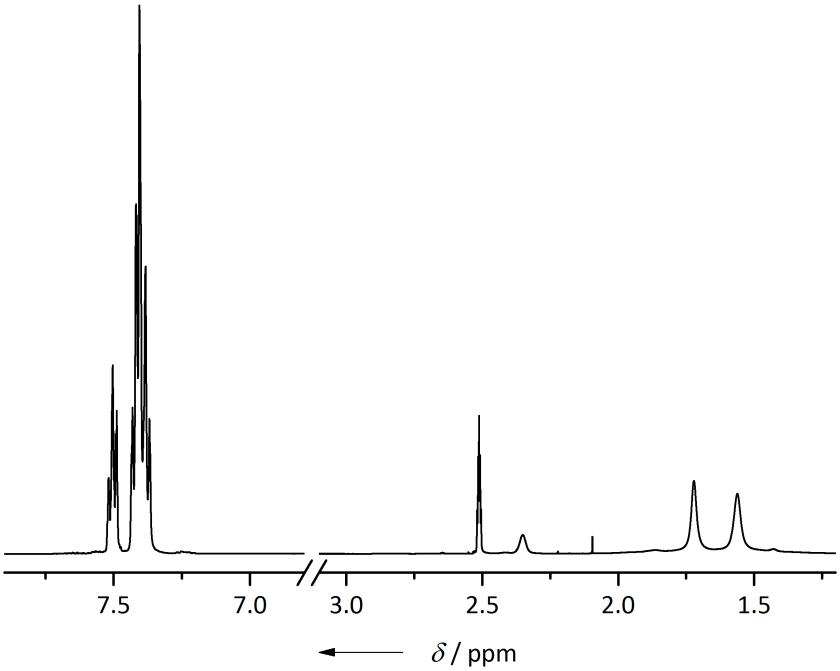

Figure S17. ^{1}H{^{11}B} NMR spectrum of **3**.

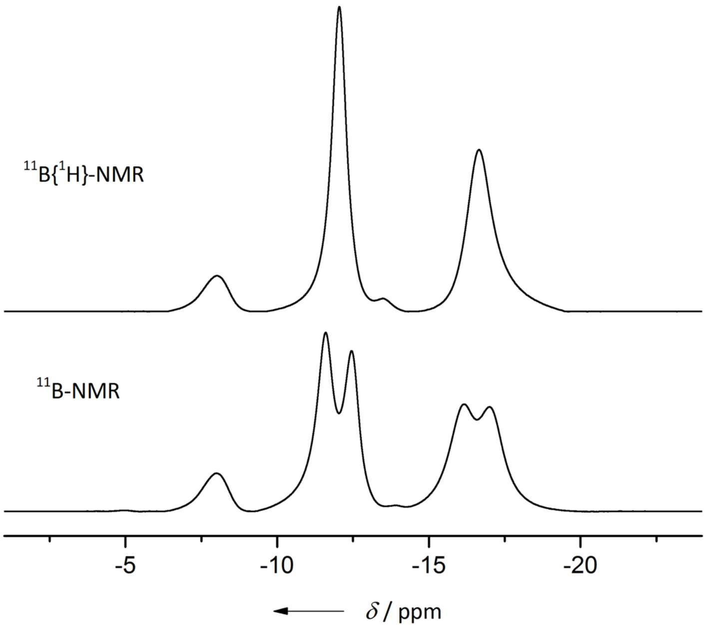

Figure S18. ^{11}B and ^{11}B{^{1}H} NMR spectra of **3**.

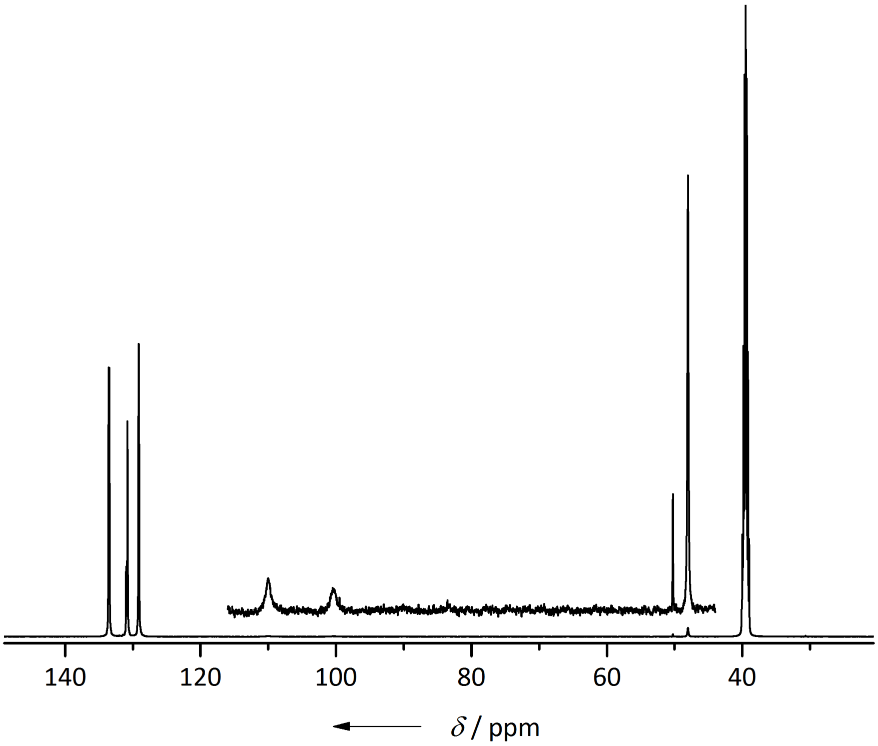

Figure S19. ^{13}C{^{1}H} NMR spectra of **3**.

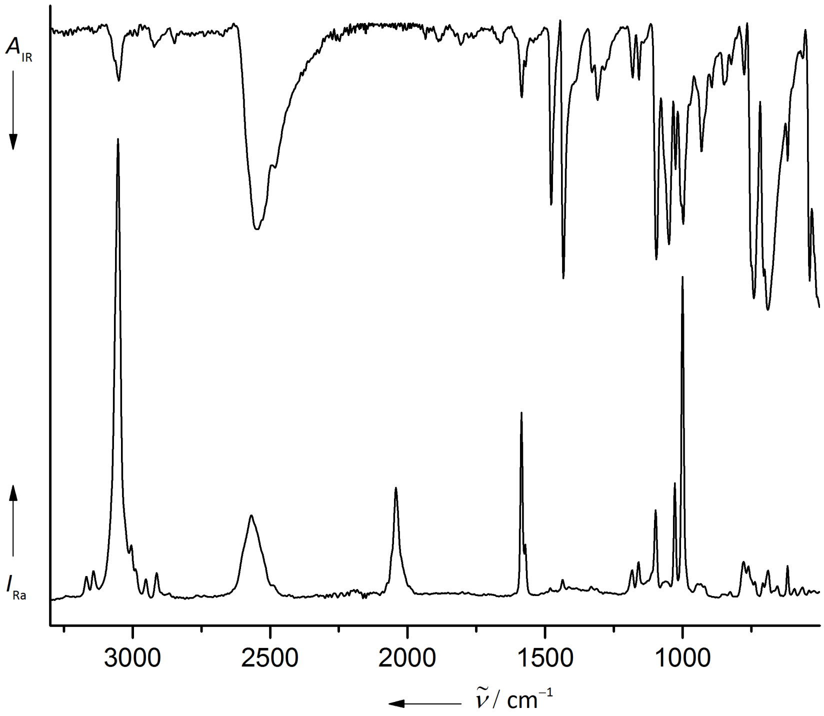

Figure S20. IR and Raman spectrum of **4**.

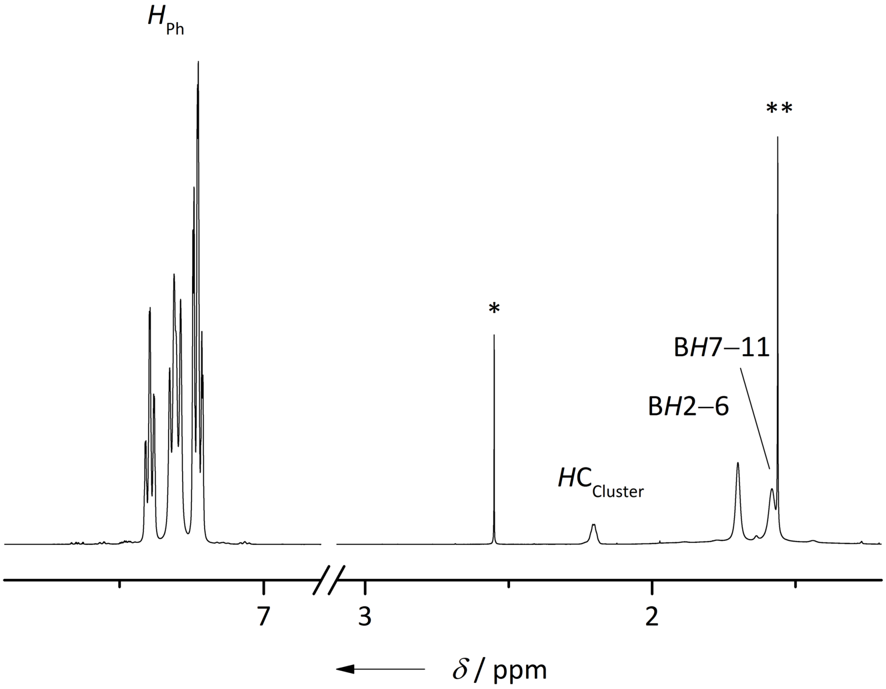

Figure S21. ^{1}H{^{11}B} NMR spectrum of **4**.

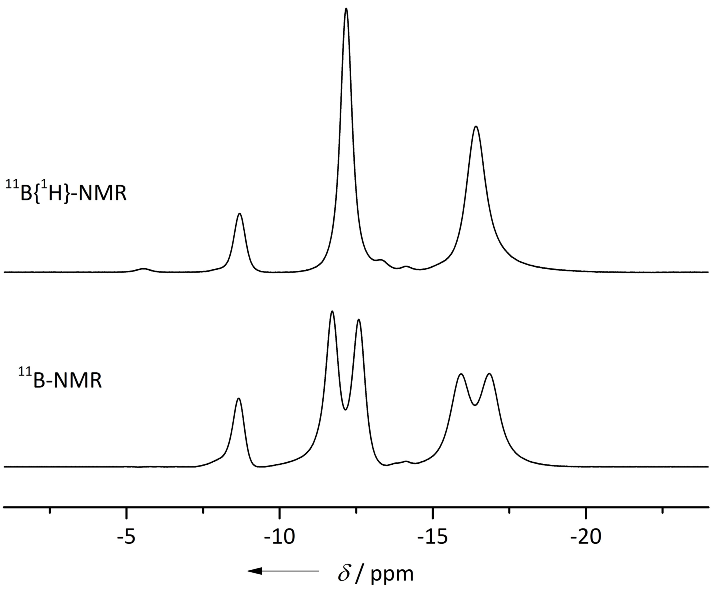

Figure S22. ^{11}B and ^{11}B{^{1}H} NMR spectra of **4**.

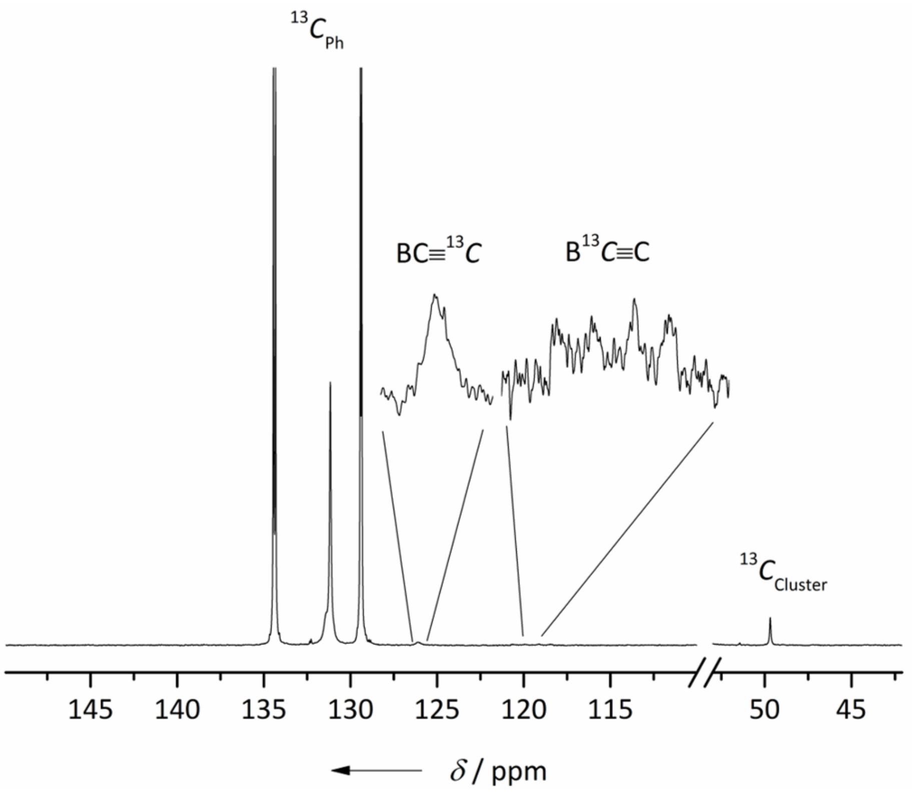

Figure S23. ^{13}C{^{1}H} NMR spectra of **4**.

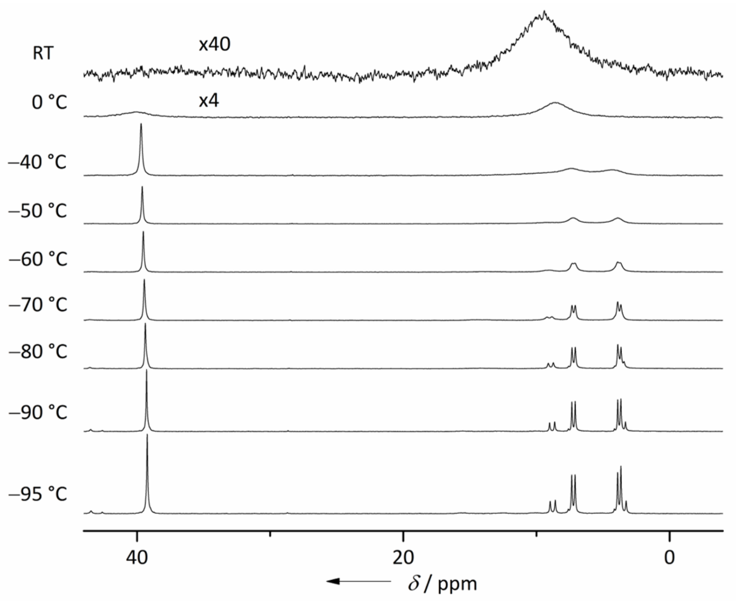

Figure S24. Temperature dependent $^{31}P\{^{1}H\}$ NMR spectra of **4** in CD_2Cl_2 (121.5 MHz).

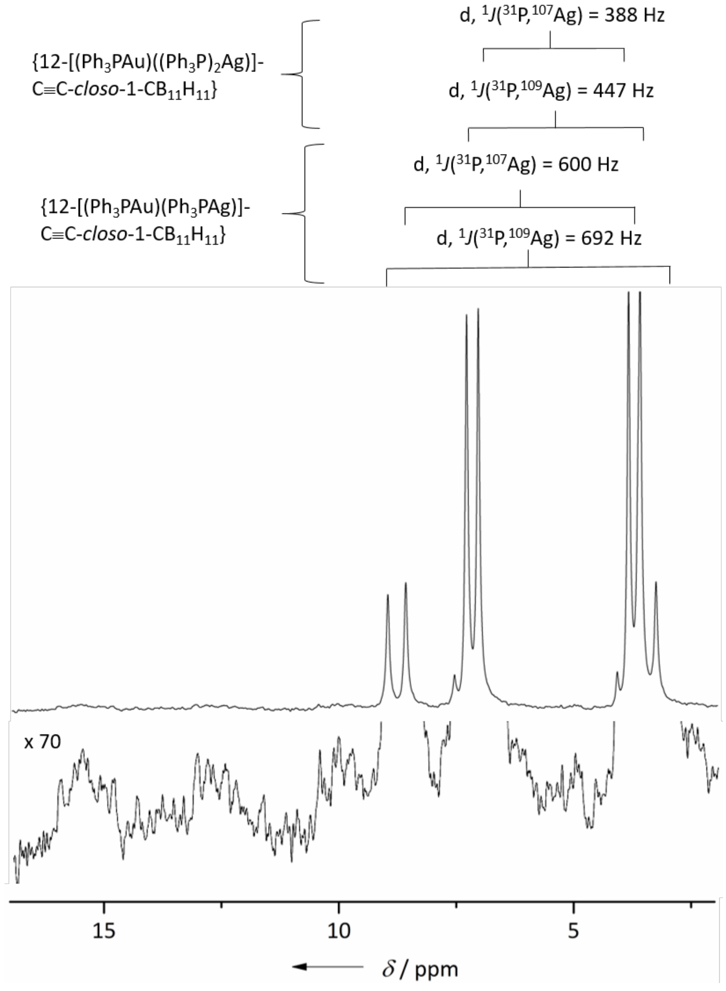

Figure S25. Section of the $^{31}P\{^{1}H\}$ NMR spectrum of **4** in CD_2Cl_2 at –90 °C (121.5 MHz) and results of the fitting of the two major components.

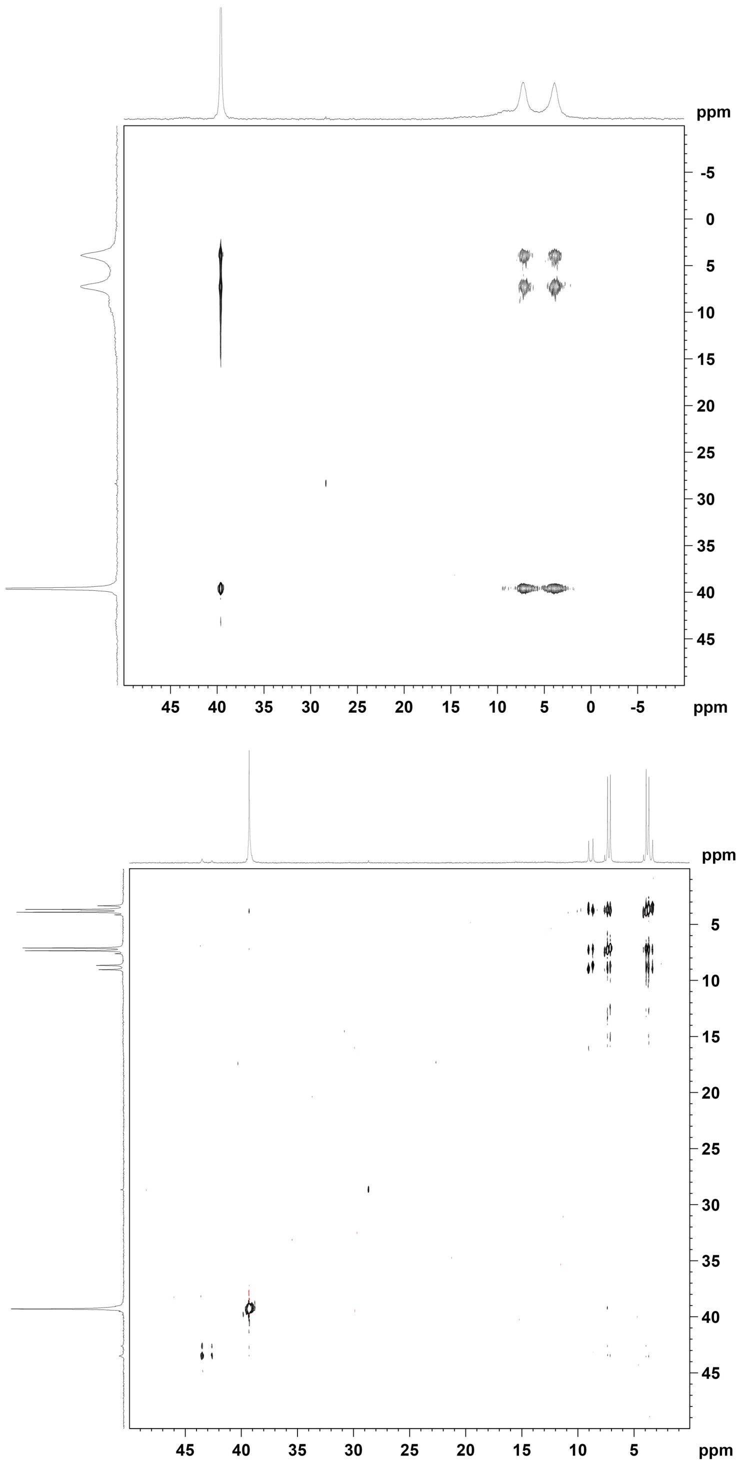

Figure S26. ^{31}P-^{31}P EXSY NMR spectra of **4** in CD_2Cl_2 at –50 (top) and –90 °C (bottom) (121.5 MHz).

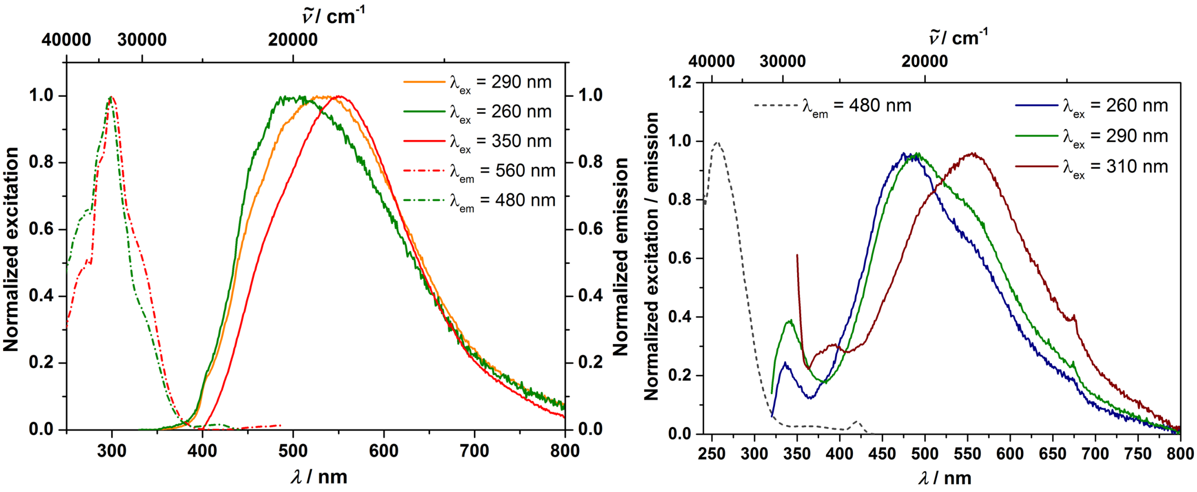

Figure S27. Left: Excitation dependent emission spectra of **1** in the solid state. Right: Excitation dependent emission spectra of **1** in THF solution.

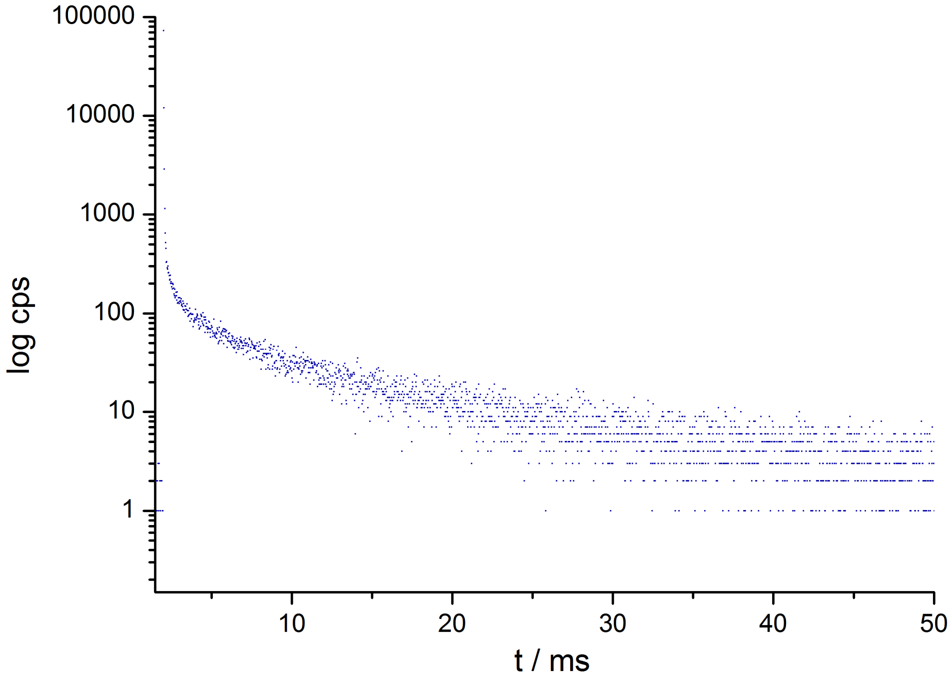

Figure S28. Emission lifetime decay of **1** at λ_{em} = 530 nm upon excitation at λ_{ex} = 300 nm in the solid state showing a long-lived component besides the sharp short-lived decay.

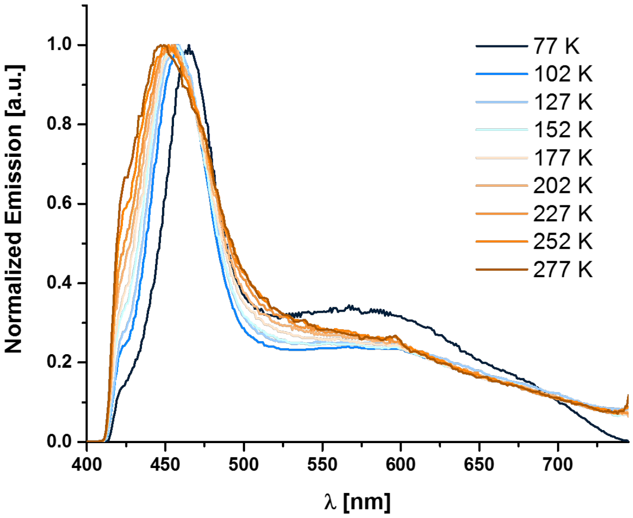

Figure S29. Normalized temperature-dependent emission spectra of **2** upon excitation at λ_{ex} = 350 nm showing that the emitting triplet states do not thermally interconvert because the relative magnitudes of the respective emissions are maintained. Thus, population discrimination must occur from the S_n states, which means during the ISC processes $S_n \rightarrow T_n$.

Table S4. Temperature-dependent lifetimes of **2** upon excitation at λ_{ex} = 376 nm.

λ_{em}	77 K	102 K	127 K	152 K	177 K	202 K	227 K	252 K	277 K
480 nm	3,39	2,90	2,62	2,76	2,59	2,71	2,63	2,55	2,62
600 nm	11,21	11,14	9,19	8,37	7,34	6,48	6,11	6,07	5,90

Explanation:

The lifetime of the triplet state at 600 nm is 5.9 µs at 277 K and reaches a plateau of ca. 11 µs between 102-77 K, meaning that no non-radiative decay occurs at those low temperatures anymore, i.e. ϕ = 1.0. Due to the relationship $\tau_{obs} = \tau_{rad} \cdot \phi$ (τ_{rad} is the intrinsic or radiative lifetime of the emitting state) we conclude that the quantum yield ϕ at room temperature is ca. 0.50 (Table 2) because the observed lifetime at RT is approximately half of the one measured at low temperature. Bearing in mind that the overall ϕ at room temperature for the emission of both states has been measured to be ϕ = 0.08 (Table 2), and that the two emitting states are not populated to equal extent (see Figure S29), the non-radiative decay must occur predominantly from the triplet state at 480 nm, of which the lifetime only starts to grow at very low temperatures (102-77 K) due to restriction of vibrational modes. This means that non-radiative decay is very efficient from that state even at low T. Because the low-energy state has ϕ = 0.50, the quantum yield of the high-energy state can be approximated to be ca. ϕ = 0.04 (Table 2).

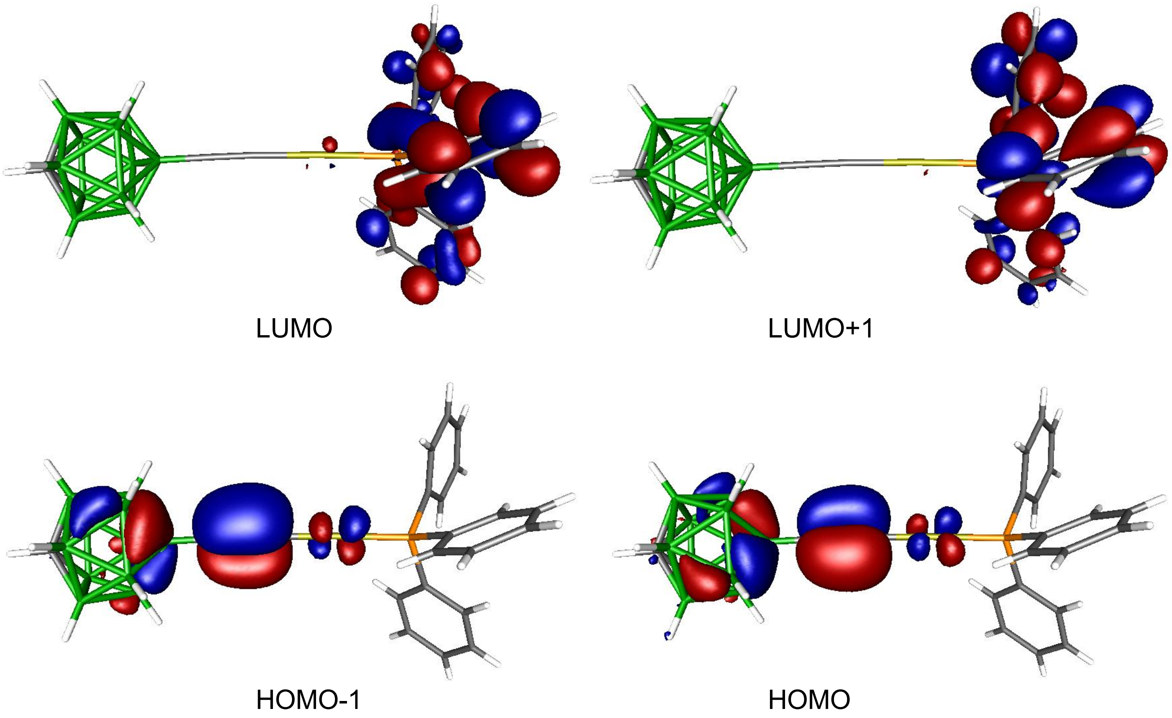

Figure S30. Selected frontier molecular orbitals of **1**.

Table S5. Selected calculated FC transitions from the ground state S_0 of **1**.

State	λ / nm	$\tilde{\nu}$ / cm^{-1}	*f*	Composition (%)
S_1	495	20212	0.0019	HOMO→LUMO (97)
S_2	479	20883	0.0222	HOMO-1→LUMO (94)
S_3	443	22586	0.0083	HOMO→LUMO+1 (93)
S_4	438	22814	0.0158	HOMO-1→LUMO+1 (30), HOMO-1→LUMO+2 (13), HOMO→LUMO+2 (54)
S_5	436	22961	0.0266	HOMO-1→LUMO+1 (47), HOMO→LUMO+2 (38)
T_1	499	20061	-	HOMO→LUMO (98)
T_2	488	20476	-	HOMO-1→LUMO (97)
T_3	451	22185	-	HOMO→LUMO+1 (64), HOMO→LUMO+2 (32)
T_4	443	22510	-	HOMO→LUMO+1 (33), HOMO→LUMO+2 (66)
T_5	439	22760	-	HOMO-1→LUMO+1 (69), HOMO-1→LUMO+2 (28)

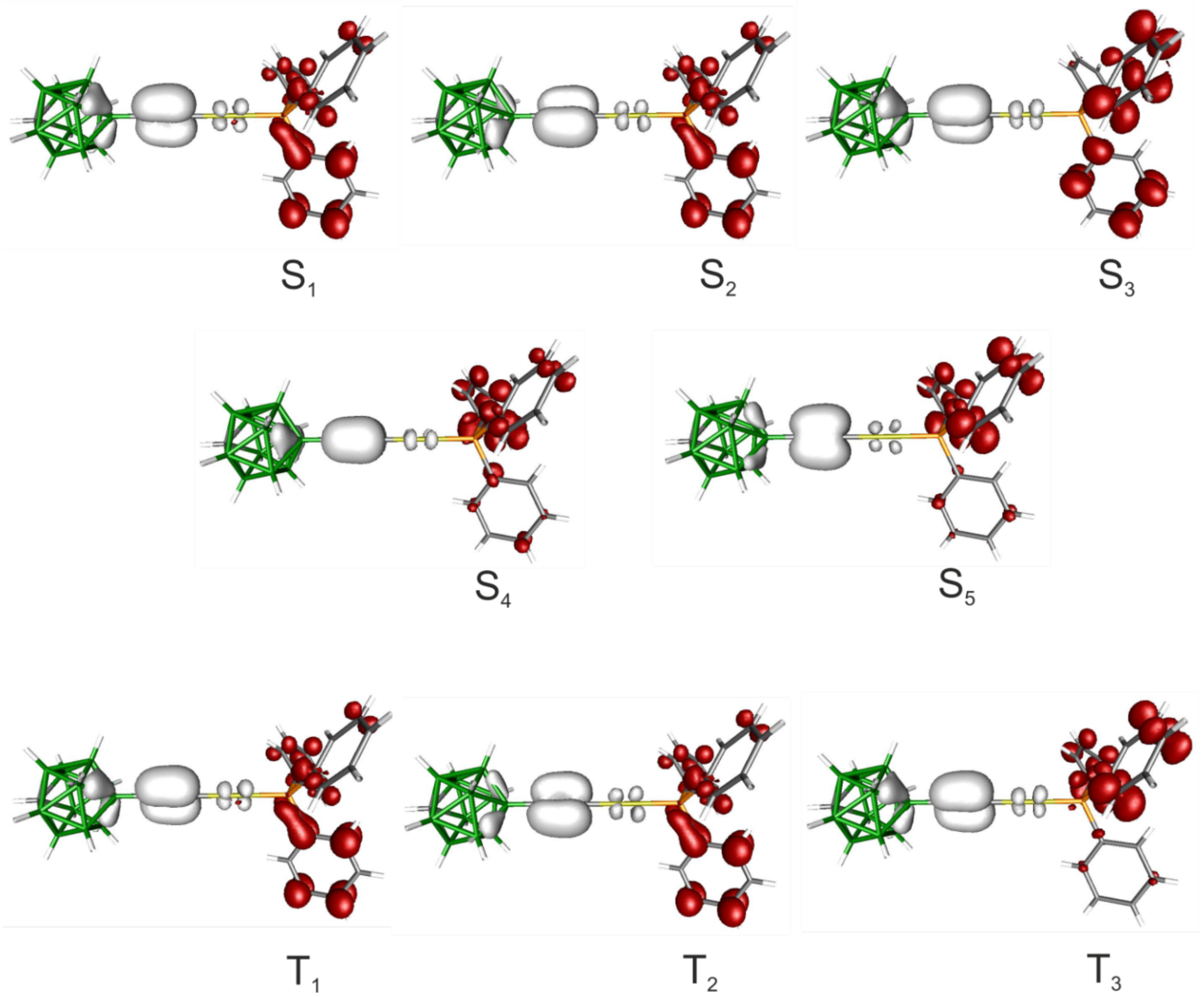

Figure S31. Calculated transition density differences of selected singlet and triplet excitations of **1**.

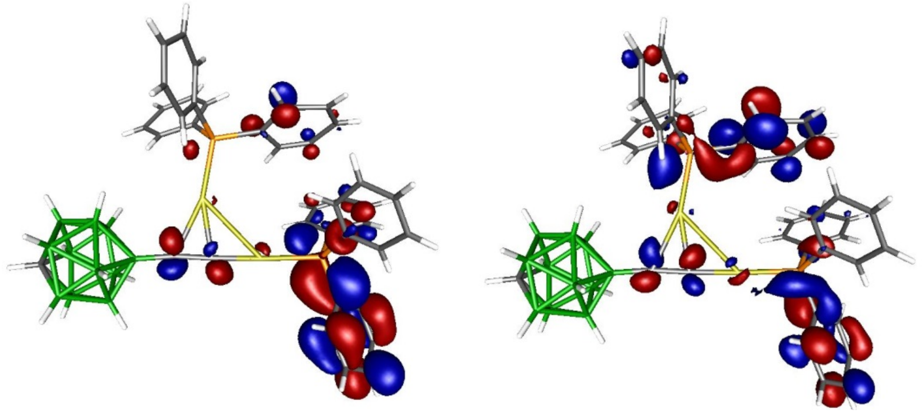

LUMO LUMO+1

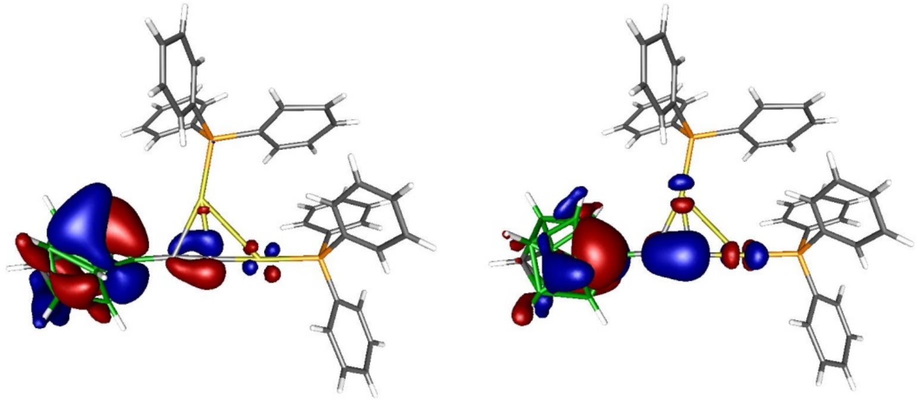

HOMO-1 HOMO

Figure S32. Selected frontier molecular orbitals of **2**.

Table S6. Selected calculated FC transitions from the ground state S_0 of **2**.

State	λ / nm	$\tilde{\nu}$ / cm^{-1}	*f*	Composition (%)
S_1	409	24431	0.0010	HOMO→LUMO (51), HOMO→LUMO+1 (28)
S_2	359	27881	0.0297	HOMO→LUMO (34), HOMO→LUMO+1 (53)
S_3	340	29372	0.0077	HOMO-1→LUMO (25), HOMO→LUMO+2 (38)
S_4	333	30016	0.0568	HOMO-1→LUMO (24), HOMO→LUMO+1 (49)
S_5	331	30193	0.0007	HOMO→LUMO+1 (12), HOMO→LUMO+3 (18), HOMO→LUMO+5 (45)
T_1	431	23181	-	HOMO→LUMO (40), HOMO→LUMO+1 (29), HOMO→LUMO+5 (11)
T_2	401	24929	-	HOMO→LUMO (16), HOMO→LUMO+9 (25)
T_3	370	27054	-	HOMO-8→LUMO+2 (22), HOMO-8→LUMO+3 (29)
T_4	364	27440	-	HOMO-1→LUMO (35), HOMO-1→LUMO+1 (20)
T_5	351	28457	-	HOMO-10→LUMO+1 (10)

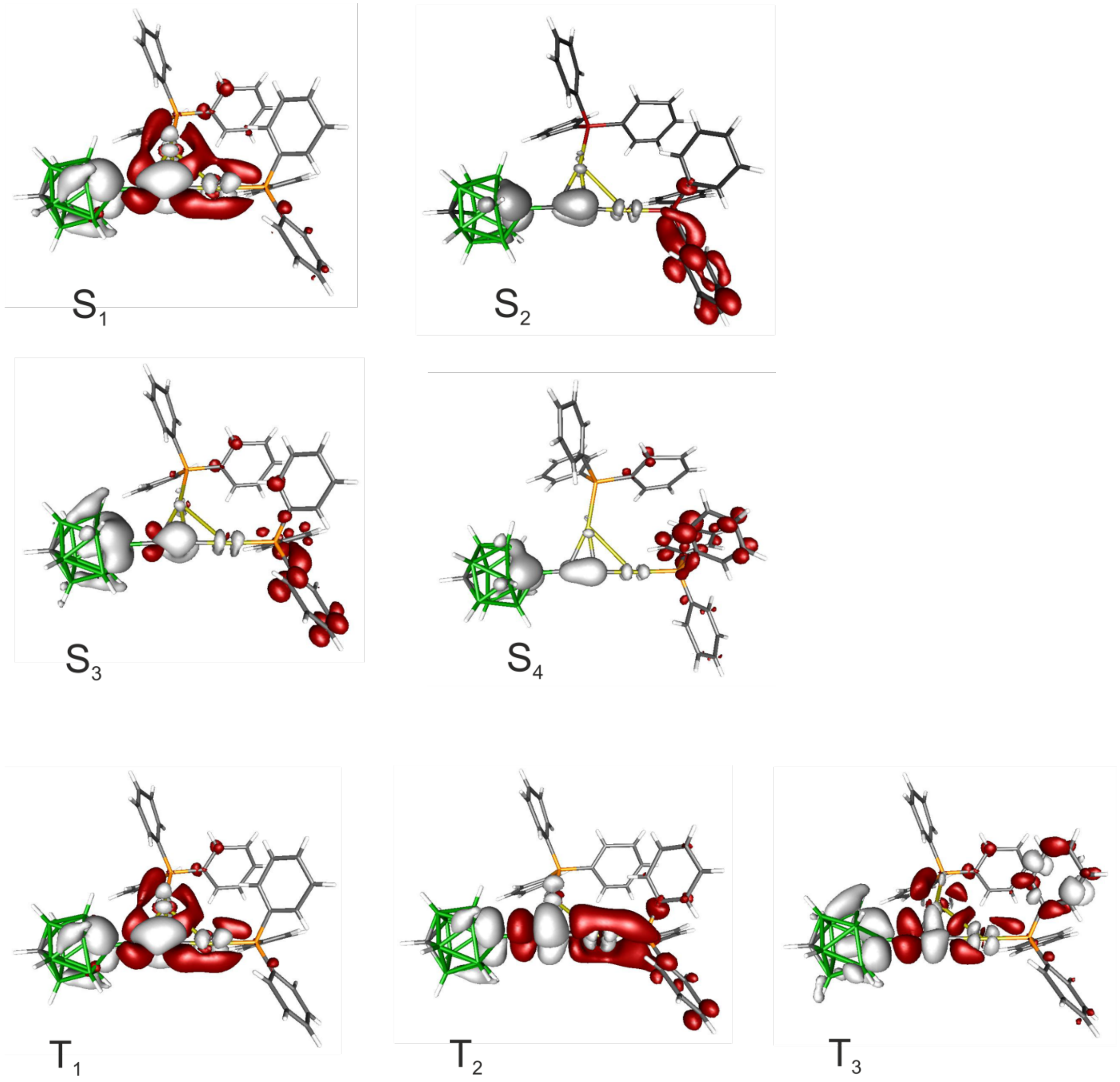

S1 S2

S3 S4

T1 T2 T3

Figure S33. Calculated transition density differences of selected singlet and triplet excitations of **2**.

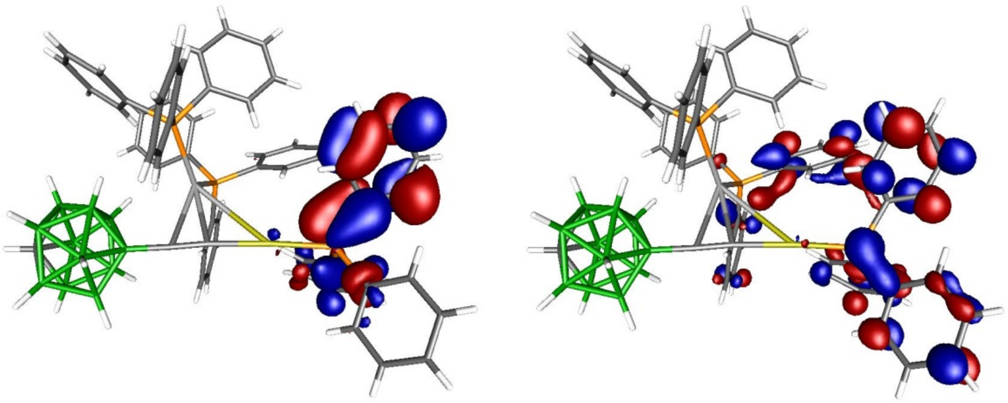

LUMO LUMO+1

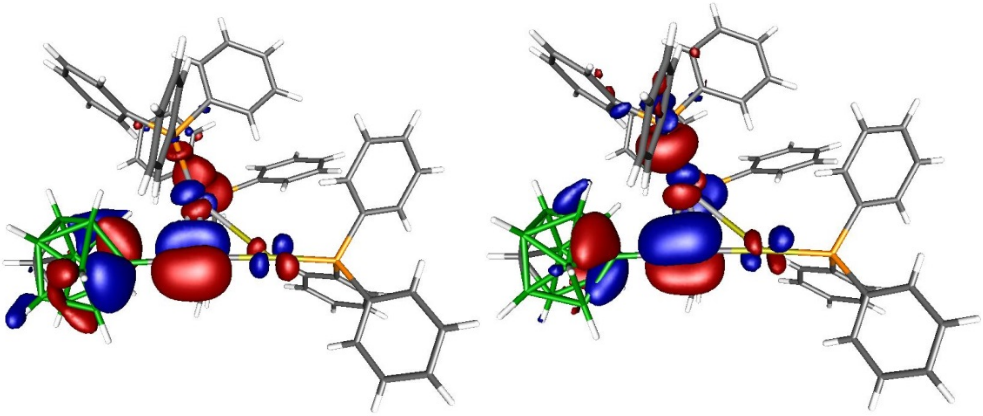

HOMO-1 HOMO

Figure S34. Selected frontier molecular orbitals of **4**.

Table S7. Selected calculated FC transitions from the ground state S_0 of **4**.

State	λ / nm	ṽ / cm^{-1}	*f*	Composition (%)
S_1	347	28783	0.0019	HOMO→LUMO (95)
S_2	329	30444	0.0118	HOMO-1→LUMO (92)
S_3	327	30563	0.0023	HOMO→LUMO+1 (55), HOMO→LUMO+2 (26)
S_4	314	31859	0.0075	HOMO-1→LUMO+1 (15), HOMO→LUMO+1 (29), HOMO→LUMO+2 (40)
S_5	309	32348	0.0064	HOMO→LUMO+4 (65)
T_1	350	28536	-	HOMO→LUMO (84)
T_2	339	29545	-	HOMO→LUMO+1 (30), HOMO→LUMO+2 (20)
T_3	336	29791	-	HOMO-1→LUMO (69), HOMO-1→LUMO+3 (11)
T_4	326	30682	-	HOMO→LUMO+6 (21), HOMO→LUMO+4 (14)
T_5	323	30951	-	HOMO→LUMO+4 (21)

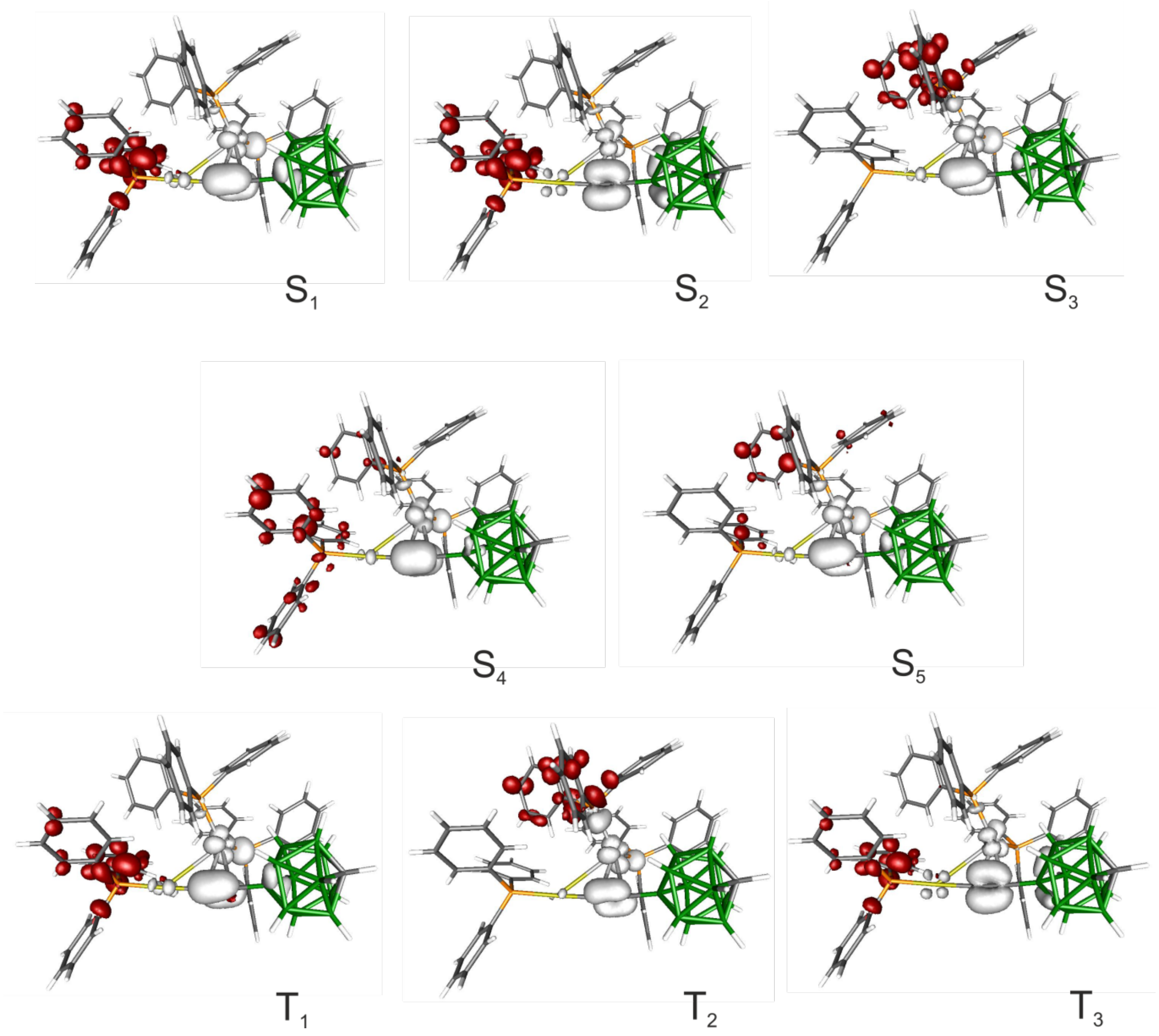

S_1 S_2 S_3

S_4 S_5

T_1 T_2 T_3

Figure S35. Calculated transition density differences of selected singlet and triplet excitations of **4**.

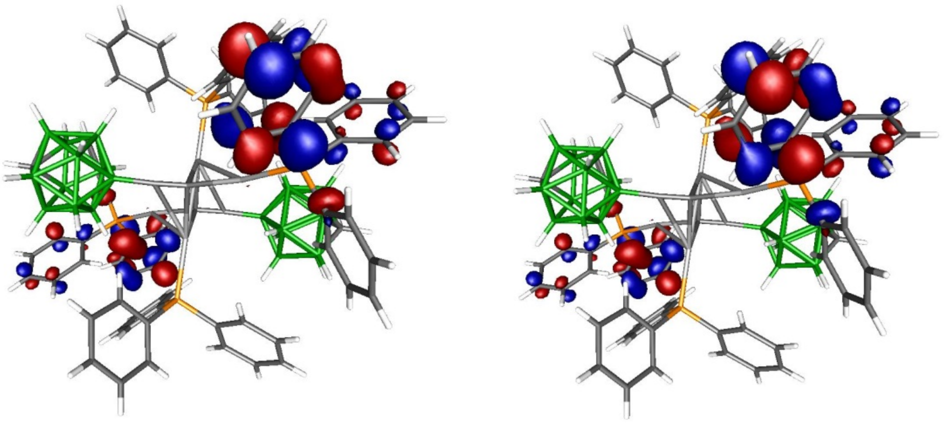

LUMO LUMO+1

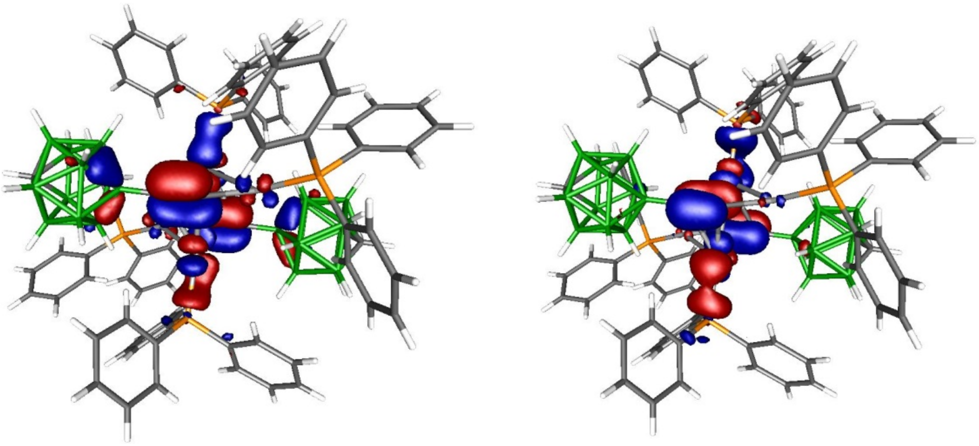

HOMO-1 HOMO

Figure S36. Selected frontier molecular orbitals of **3**.

Table S8. Selected calculated FC transitions from the ground state S_0 of **3**.

State	λ / nm	ṽ / cm^{-1}	*f*	Composition (%)
S_1	311	32121	0.0000	HOMO→LUMO+1 (14), HOMO→LUMO+2 (33), HOMO→LUMO+4 (43)
S_2	307	32624	0.0093	HOMO→LUMO (56), HOMO→LUMO+5 (23)
S_3	303	32999	0.0000	HOMO→LUMO+1 (83), HOMO→LUMO+2 (12)
S_4	302	33124	0.0466	HOMO→LUMO (32), HOMO→LUMO+5 (53)
S_5	301	33259	0.0181	HOMO→LUMO+3 (84)
T_1	332	30083	-	HOMO→LUMO+2 (17), HOMO→LUMO+4 (30)
T_2	330	30344	-	HOMO→LUMO+5 (33)
T_3	321	31143	-	HOMO→LUMO+8 (16)
T_4	320	31210	-	HOMO→LUMO+9 (14)
T_5	315	31787	-	HOMO→LUMO (15), HOMO→LUMO+2 (19), HOMO→LUMO+10 (11)

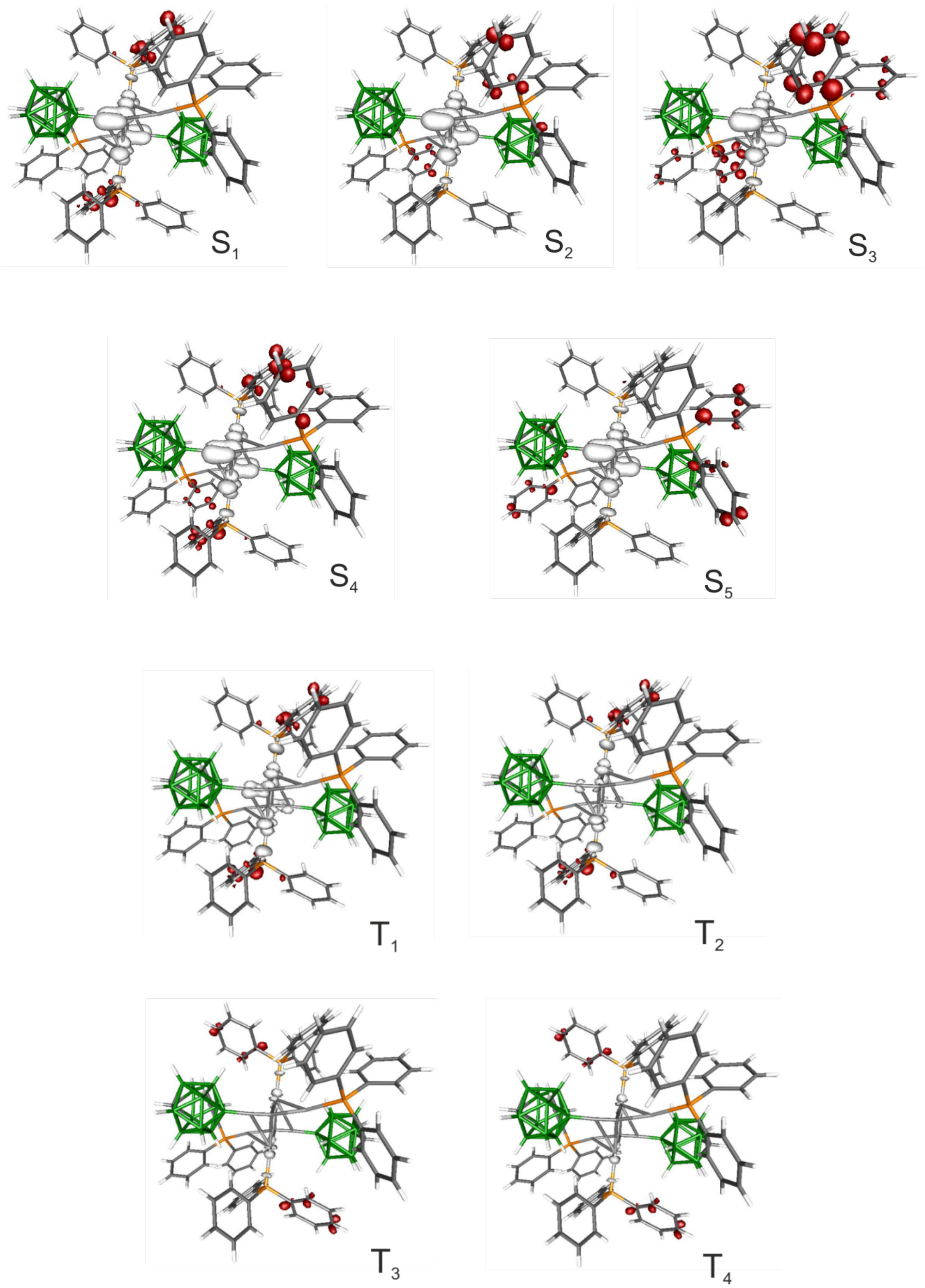

Figure S37. Calculated transition density differences of selected singlet and triplet excitations of **3**.

Table S9. Cartesian coordinates used for DFT and TD-DFT calculations obtained from single crystal X-ray diffraction experiments of **1**.

Au	5.723180	3.604410	9.986350
C	3.924740	3.248970	9.179760
P	7.797690	3.979620	10.867120
C	8.031150	3.342340	12.555460
C	7.253940	2.280800	12.996090
C	8.963410	3.918890	13.402450
C	9.106110	3.237180	9.852940
C	9.031450	3.348680	8.477200
C	10.183400	2.515590	10.411070
C	8.226270	5.745520	11.020600
C	11.118040	1.939050	9.586110
C	11.056430	2.038760	8.232410
H	11.822260	1.463120	9.967990
B	0.688990	1.087820	8.340120
B	-0.126820	0.562040	6.920310
B	1.311810	1.432300	6.729370
B	1.471120	2.649760	8.007200
B	-0.026650	2.577240	8.988820
B	-1.072410	1.323520	8.283810
H	1.145760	0.346290	9.015750
C	9.992050	2.754010	7.666930
H	9.931800	2.831970	6.741610
C	7.592370	6.472550	12.009570
C	9.225940	6.327510	10.254400
C	-1.359440	1.809410	6.734270
B	-1.370910	3.000580	7.943550
H	-1.791580	0.738810	8.881110
B	-0.070170	1.837520	5.689000
H	-0.183320	-0.499490	6.655940
C	9.614360	7.684570	10.477160
H	9.648140	5.830740	9.588560
B	-0.736900	3.317860	6.403800
B	0.178900	3.840930	7.772190
H	-2.269270	3.511860	8.320530
C	7.953720	7.824170	12.212750
C	8.916700	8.388940	11.441650
H	7.532580	8.325480	12.876140
B	1.002250	3.127490	6.340150
H	1.658500	3.709480	5.679210
H	-1.232250	4.073900	5.772230
H	8.330410	3.824610	8.087980
H	10.257660	2.429470	11.333940
C	2.850890	3.001490	8.658350
H	11.704750	1.642610	7.693860
C	8.355380	2.395030	15.150270
C	9.117400	3.455650	14.692510
C	7.424150	1.780410	14.293490
H	8.460640	2.089530	16.024190
H	9.735310	3.859060	15.257980
H	9.119060	9.288200	11.564050
H	10.306140	8.078000	9.994920
H	-2.321760	1.512080	6.291190
H	0.317430	4.897020	8.048810
H	-0.025930	2.804770	10.065910
H	6.620920	1.901880	12.428170
H	-0.147430	1.602730	4.616810
H	2.200290	0.924650	6.323020
H	9.490120	4.623250	13.098900
H	6.928640	1.049750	14.584800
H	6.936430	6.077310	12.535880

Table S10. Cartesian coordinates used for DFT and TD-DFT calculations obtained from single crystal X-ray diffraction experiments of **2**.

Au	7.925440	5.775940	7.732630
C	7.927500	4.447170	6.464300
P	7.856510	7.477380	9.254990
Au	7.480530	5.660890	4.633450
C	8.326500	-0.284820	2.312430
B	6.929730	0.495590	2.364990
B	8.365330	1.286110	1.576660
B	9.734870	0.751760	2.435060
B	7.440170	-0.444080	3.801500
B	9.240070	-0.318430	3.801500
H	8.335040	-1.166860	1.651990
P	7.172940	7.442030	3.288210
C	8.052500	3.498230	5.465750
B	9.600990	1.425440	4.239460
B	8.276140	0.647560	5.045310
H	9.903530	-1.147310	4.087050
B	9.119820	2.363890	2.785430
H	10.678150	0.585610	1.884980
C	8.179350	6.900200	10.861430
C	6.322880	8.335640	9.162140
C	9.132870	8.764100	8.916880
B	7.395990	2.228500	2.645280
B	6.761740	1.142770	4.116830
H	6.048270	0.202120	1.774620
H	8.423470	1.499110	0.499280
B	8.085560	2.359960	4.537270
H	10.477880	1.738080	4.826330
H	6.909470	-1.348900	4.144860
C	3.328010	7.464580	0.735770
H	4.156260	9.166980	-0.080580
C	5.686980	7.441180	2.207320
C	4.587690	6.593730	2.505140
H	8.308340	0.424160	6.120940
H	5.777790	1.261380	4.607350
C	3.415870	6.584650	1.716810
H	2.725020	5.979860	1.890240
H	6.211170	9.004760	1.037090
H	2.593280	7.427060	0.162920
C	4.367220	9.252290	10.353390
H	3.984570	9.450120	11.178510
H	2.837110	9.863980	9.177900
H	6.134260	8.496800	11.054130
H	4.634470	6.029400	3.244410
C	8.540970	7.592580	2.084690
C	7.213170	8.989830	4.274500
C	10.174060	8.551080	7.988400
C	9.039290	9.994680	9.530030
C	8.878290	6.370980	1.436510
C	9.155730	8.727280	1.646730
C	8.314310	9.421560	5.062830
C	6.125730	9.885680	4.344570
C	11.120260	9.556770	7.830740
H	10.227790	7.765790	7.487380
H	8.319040	10.147080	10.095870
C	9.976280	11.044840	9.354840
C	10.187800	8.746380	0.770810

C	9.044160	7.448130	11.842460
C	9.247960	6.963410	13.086270
H	9.511730	8.211880	11.605960
H	9.676240	3.259600	2.475350
H	6.820100	3.058820	2.216080
C	7.462950	5.765500	11.299390
C	7.606340	5.265230	12.648310
H	6.893470	5.323120	10.719530
C	8.504390	5.874400	13.524230
H	9.874740	7.360550	13.639850
C	4.294400	9.290670	8.111030
C	3.701120	9.524840	9.179660
C	5.564780	8.569810	8.093510
H	3.931050	9.583200	7.306940
H	5.870010	8.237920	7.278910
C	5.691140	8.662420	10.248280
H	7.103260	4.544630	12.930350
H	8.608830	5.551980	14.391390
C	4.321350	8.478040	0.525550
C	5.522190	8.412500	1.226290
H	8.851970	9.536430	1.981330
H	9.059600	8.867300	5.059320
C	8.375040	10.475460	5.763560
C	6.054870	11.055310	5.395680
H	5.423880	9.787350	3.734930
C	10.985980	10.751870	8.426360
H	11.864650	9.397780	7.301680
H	9.913630	11.859240	9.798060
C	10.548170	7.577780	0.227740
H	10.615810	9.541340	0.539570
H	9.182540	10.714460	6.145460
C	7.182250	11.335360	5.973780
H	11.592490	11.424670	8.212640
H	8.391320	5.597460	1.630970
C	9.887620	6.306470	0.508030
H	5.261780	11.498810	5.597140
H	11.275050	7.579140	-0.360880
H	7.253880	12.091110	6.509850
H	10.145110	5.518480	0.099850

Table S11. Cartesian coordinates used for DFT and TD-DFT calculations obtained from single crystal X-ray diffraction experiments of **3**.

Ag	15.576670	1.652810	11.842140
C	16.142860	0.480210	9.880350
P	14.339280	3.457890	12.808870
C	16.831120	0.219140	13.408080
C	15.139840	-0.194280	10.083890
Ag	17.397310	-0.953460	11.446280
C	11.427260	-3.112400	10.831680
B	12.243870	-2.503360	12.192190
B	11.314760	-2.035920	9.516120
B	12.421710	-3.418150	9.476760
B	12.998850	-3.715040	11.132800
B	11.207600	-1.452640	11.195440
H	10.563340	-3.801560	11.013090
Ag	17.683200	1.487790	8.895690
P	19.052880	2.476760	7.223600
B	12.812690	-0.893970	11.693350
B	12.228430	-0.602960	10.022400
H	10.268470	-0.998650	11.602290
B	13.910270	-1.126000	10.303960
B	13.922340	-2.299490	11.647940
H	11.982620	-2.740560	13.255770
B	14.030820	-2.873600	9.957200
H	13.234910	-4.746610	11.499820
C	20.838550	2.179770	7.359840
C	18.874270	4.283960	7.088060
C	18.588320	1.850760	5.574550
B	12.977580	-1.820370	8.953700
H	10.438920	-1.971210	8.819330
C	12.886910	3.953110	11.845420
C	13.720210	3.067630	14.474220
C	15.295330	4.993250	13.017760
H	12.276890	-4.260940	8.751790
H	13.216700	-1.592890	7.883130
H	14.963530	-3.338520	9.548250
H	14.786660	-2.387020	12.354510
H	12.948340	-0.059020	12.429030
H	11.976890	0.424520	9.655380
C	15.372460	5.687440	14.217120
C	16.019760	5.453780	11.913430
C	16.176200	6.819930	14.314230
H	14.875790	5.389310	14.972130
C	16.886180	7.272230	13.216180
H	16.238960	7.285140	15.139800
H	23.783040	3.288750	6.492810
H	21.510970	3.808260	6.320480
C	17.834140	0.893630	13.204540
B	19.063710	1.825340	12.984460
P	18.634700	-2.758550	10.479560
Ag	15.290780	-0.788440	14.392730
B	19.996390	2.519720	14.334720
B	18.943150	3.572950	13.331220
B	19.051630	2.998840	11.640480
B	20.161280	1.593320	11.595070
B	20.745550	1.302310	13.266020
C	17.678650	-4.293900	10.270660
C	20.087060	-3.253760	11.443000
C	19.253760	-2.368280	8.814200
P	13.921100	-1.777410	16.064820
B	21.659220	2.735270	13.772310
B	20.552260	4.117500	13.811660
H	19.757280	2.292240	15.405290
B	19.975120	4.414390	12.155630
H	18.010440	4.037870	13.740170
B	20.730100	3.202700	11.096230
H	18.187320	3.086370	10.933910
B	21.766380	2.151990	12.092980
H	20.025630	0.758360	10.859390
H	20.997080	0.274830	13.633040
C	17.601520	-4.988090	9.071310
C	16.954210	-4.754430	11.375000
C	20.681910	-2.316930	12.244120
C	20.646700	-4.511080	11.376390
C	20.591970	-2.515210	8.447880
C	18.335140	-1.889470	7.874750
C	14.099700	-3.584610	16.200360
C	14.385660	-1.151410	17.713870
C	12.135430	-1.480420	15.928580
C	21.546710	3.811750	12.456740
H	22.535050	2.670560	14.469100
H	20.697090	4.960290	14.536630
H	19.739070	5.445950	11.788600
H	20.991360	3.439910	10.032650
H	22.705510	1.698000	11.686130
H	18.098180	-4.689970	8.316300
C	16.797780	-6.120580	8.974190
C	16.172710	-5.896440	11.278120

C	16.801260	6.595780	12.010310
H	17.431250	8.046480	13.288370
H	17.276450	6.914160	11.250640
H	15.977490	4.980480	11.089950
C	12.292060	3.016280	11.044300
C	12.327270	5.210420	11.912030
C	11.166880	3.315930	10.294880
H	12.659260	2.142320	11.001450
C	10.645520	4.578110	10.319800
H	10.757040	2.643400	9.762510
C	11.197110	5.516930	11.164470
H	9.912260	4.804690	9.762510
H	10.801590	6.378100	11.234330
H	12.717530	5.871520	12.470950
C	12.382010	3.214560	14.840550
C	14.638830	2.588820	15.413670
C	11.983320	2.893180	16.133750
H	11.746220	3.531390	14.210590
C	12.900950	2.457520	17.061800
H	11.069130	2.975300	16.378750
C	14.230870	2.300120	16.708980
H	12.622230	2.265300	17.948390
H	14.861940	1.995860	17.349870
H	15.546170	2.460320	15.163090
C	18.805460	4.931030	5.867290
C	18.812400	5.033870	8.250860
C	18.709030	6.413220	8.194030
H	18.841830	4.597030	9.094130
C	18.633520	7.048380	6.984200
H	18.688960	6.919860	8.996320
C	18.684360	6.310750	5.823040
H	18.547740	7.993270	6.944610
H	18.636920	6.751790	4.983720
H	18.841120	4.431050	5.060570
C	19.512300	1.438430	4.626710
C	17.226080	1.753150	5.284380
C	16.804490	1.278710	4.060800
H	16.586090	2.017330	5.933890
C	17.722760	0.865760	3.119480
H	15.875480	1.234800	3.865880
C	19.072400	0.938260	3.406400
H	17.430160	0.533350	2.279940
H	19.706580	0.644330	2.762010
H	20.442420	1.496990	4.811390
C	21.254650	1.054680	8.052440
C	21.786950	3.025620	6.783450
C	22.612030	0.765510	8.155140
H	20.613900	0.481010	8.458350
C	23.541100	1.587890	7.566870
H	22.896600	-0.004460	8.633020
C	23.134360	2.717520	6.889410
H	24.464860	1.377650	7.626960
H	16.996480	-4.281130	12.198480
H	20.314710	-1.442970	12.286970
C	21.807100	-2.616580	12.993540
C	21.776870	-4.817580	12.123950
H	20.256450	-5.172170	10.817470
H	21.227750	-2.832040	9.077830
C	20.990650	-2.193830	7.154670
C	18.743100	-1.600780	6.579440
H	17.427810	-1.760970	8.125330
C	14.161570	-4.334530	15.037570
C	14.168510	-4.231680	17.421140
C	15.747890	-1.053800	18.004050
C	13.461680	-0.739080	18.661710
C	11.719320	-0.355330	15.235980
C	11.187030	-2.326270	16.504970
H	22.410640	4.500900	12.275330
H	16.735020	-6.585790	8.148620
C	16.087800	-6.572880	10.072240
H	15.697530	-6.214810	12.037790
H	22.216940	-1.944050	13.525920
C	22.328450	-3.878760	12.968620
H	22.172380	-5.678750	12.054090
H	21.904850	-2.275950	6.909670
C	20.073020	-1.758180	6.226620
H	18.112040	-1.296510	5.938550
H	14.132150	-3.897690	14.194290
C	14.264940	-5.713870	15.094390
C	14.289610	-5.611400	17.465390
H	14.132860	-3.731700	18.227850
H	16.387880	-1.317980	17.354530
C	16.169490	-0.579360	19.227620
C	13.901580	-0.238920	19.882020
H	12.531560	-0.797640	18.477030
H	12.360080	0.218340	14.830070
C	10.361950	-0.066160	15.133280
C	9.839610	-2.018170	16.399010
H	11.463010	-3.108920	16.967950
H	15.542730	-7.347130	10.000050
H	23.061720	-4.105340	13.525920
H	20.351750	-1.565950	5.340040
H	14.285020	-6.220510	14.292100
C	14.340450	-6.349030	16.304220
H	14.337060	-6.052440	18.304700
H	17.098500	-0.535450	19.422540
C	15.251210	-0.166410	20.168940
H	13.267400	0.055010	20.526410
H	10.077380	0.703800	14.655400
C	9.432880	-0.888550	15.721550
H	9.190940	-2.589400	16.795610
H	14.426230	-7.293920	16.343810
H	15.543820	0.166000	21.008480
H	8.509120	-0.678300	15.661460

Table S12. Cartesian coordinates used for DFT and TD-DFT calculations obtained from single crystal X-ray diffraction experiments of **4**.

P	9.874600	7.823570	15.056330
C	9.606290	9.485600	15.727540
C	10.933480	6.899190	16.206980
C	8.279090	6.949660	15.204980
Au	10.799120	7.761320	12.972680
C	11.725290	7.561560	11.212210
Ag	13.432800	9.229480	11.463090
P	15.054150	9.087540	13.294340
C	16.535610	9.977640	12.729160
C	14.650460	9.834660	14.903110
C	15.647390	7.405960	13.708330
H	15.528420	4.237080	7.541610
C	18.607430	11.386500	11.509010
C	17.676140	12.050970	12.267480
C	18.535640	10.004980	11.374560
H	19.286420	11.859620	11.085380
H	12.742740	4.623990	8.406620
H	17.741780	12.971990	12.379100
H	11.735540	7.050590	7.082470
H	15.977650	11.798640	13.370950
H	13.362230	9.334200	7.970310
H	19.175650	9.550780	10.877370

P	13.063360	11.325940	10.194240
C	13.120180	12.610310	11.468420
C	11.485280	11.607290	9.322370
C	14.338660	11.886960	9.015430
C	12.408370	7.307130	10.238120
C	15.403290	6.558540	6.630930
B	15.460720	8.064120	7.379260
B	14.102760	7.582590	6.321460
B	13.883270	5.845700	6.488880
B	16.057660	6.602700	8.185930
B	15.085330	5.238000	7.643080
H	16.106890	6.398730	5.801430
B	13.337620	7.021150	9.025580
C	10.851430	10.528570	8.716100
C	10.935530	12.883670	9.175240
C	9.706800	10.730440	7.952550
H	11.194000	9.670640	8.822640
C	9.189870	12.011020	7.807960
H	9.288330	10.009190	7.539070
C	9.786800	13.070820	8.429450
H	8.432940	12.147700	7.285400
H	9.417560	13.920340	8.350820
C	14.065830	12.658680	7.906890
C	15.653550	11.609390	9.329980
H	11.345800	13.613330	9.583650
C	16.685350	12.143500	8.566440
H	15.850470	11.060570	10.055480
C	16.408430	12.946760	7.480730
H	17.569470	11.960560	8.789670
C	15.099690	13.182270	7.135740
H	17.101770	13.325250	6.988610
H	14.904820	13.695340	6.382340
H	13.181720	12.831100	7.670980
C	13.819670	13.798380	11.326370
C	12.549910	12.339050	12.706330
C	13.932500	14.681540	12.399390
C	13.343770	14.387150	13.604320
H	14.406350	15.474280	12.300460
H	14.217630	14.008650	10.512080
C	12.650430	13.222220	13.748910
H	13.417620	14.978030	14.317140
B	13.782750	8.320660	7.889140
B	12.796070	6.941240	7.351360
H	13.903780	8.097770	5.370190
H	12.244270	13.024560	14.560660
B	13.403260	5.467200	8.158030
H	13.544800	5.238000	5.636550
C	16.617660	11.344440	12.873750
C	17.507930	9.308960	11.983370
B	15.001230	7.696140	9.053480
H	16.133550	8.892610	7.117980
H	12.090420	11.540000	12.833170
B	14.759180	5.938220	9.218370
H	17.122280	6.489150	8.437060
H	14.966360	5.402020	10.154410
H	17.466900	8.383740	11.894590
H	15.370470	8.299630	9.898200
C	15.062770	6.331440	13.137570
C	15.499700	5.040340	13.414070
H	14.355070	6.457610	12.549060
C	16.695610	7.187270	14.608860
C	16.539710	4.857400	14.304450
H	15.095590	4.308580	13.003120
C	17.132540	5.912990	14.880280
H	16.831000	3.997370	14.504850
H	17.840240	5.782620	15.468800
H	17.101770	7.912720	15.024870
C	13.327360	9.998670	15.255710
C	15.618670	10.200540	15.839160
C	12.960180	10.488620	16.468260
H	12.664790	9.765260	14.644370
C	13.934550	10.820850	17.406840
H	12.059650	10.604270	16.671190
C	15.280210	10.671560	17.077060
H	13.688390	11.140480	18.246480
H	15.942780	10.890250	17.690940
H	16.517150	10.122740	15.613390
C	12.254530	6.630030	15.849300
C	13.054540	5.824670	16.645830
H	12.603250	6.991710	15.065460
C	10.455530	6.350370	17.386540
C	12.549910	5.290570	17.800020
H	13.932500	5.650140	16.397230
C	11.245280	5.555520	18.177990
H	13.087360	4.748050	18.332730
H	10.904760	5.195940	18.964370
H	9.579620	6.524900	17.647820
C	7.154970	7.538430	15.722470
C	8.231910	5.629120	14.829550
C	7.070870	4.895250	14.989360
H	8.986790	5.223280	14.466800
C	5.954950	5.488230	15.516990
H	7.048300	3.999470	14.740760
C	5.998030	6.791950	15.882280
H	5.171350	4.998280	15.623540
H	5.239050	7.191470	16.242490
H	7.167280	8.436310	15.968530
C	9.651410	10.553800	14.859990
C	9.341670	9.729520	17.069460
C	9.132430	11.008000	17.533670
H	9.306790	9.016680	17.663040
C	9.185770	12.065690	16.661050
H	8.953970	11.153090	18.434200
C	9.440130	11.849110	15.324200
H	9.050380	12.932040	16.973060
H	9.468850	12.568260	14.733150
H	9.823720	10.406610	13.956920

References

1. R. K. Harris, E. D. Becker, S. M. Cabral de Menezes, R. Goodfellow and P. Granger, *Pure Appl. Chem.*, 2001, **73**, 1795–1818.
2. D. C. Finster, W. C. Hutton and R. N. Grimes, *J. Am. Chem. Soc.*, 1980, **102**, 400–401.
3. I. J. Colquhoun and W. McFarlane, *J. Chem. Soc., Dalton Trans.*, 1981, 2014–2016.
4. T. L. Venable, W. C. Hutton and R. N. Grimes, *J. Am. Chem. Soc.*, 1982, **104**, 4716–4717.
5. T. L. Venable, W. C. Hutton and R. N. Grimes, *J. Am. Chem. Soc.*, 1984, **106**, 29–37.
6. W. L. F. Armarego and C. L. L. Chai, *Purification of Laboratory Chemicals*, Butterworth-Heinemann (Elsevier), 2003.
7. M. I. Bruce, B. K. Nicholson, O. B. Shawkataly, J. R. Shapley and T. Henly, *Inorg. Synth.*, 1989, **26**, 324–326.
8. A. Himmelspach, G. J. Reiss and M. Finze, *Inorg. Chem.*, 2012, **51**, 2679–2688.
9. A. Himmelspach and M. Finze, *J. Organomet. Chem.*, 2010, **695**, 1337–1345.
10. M. Hailmann, N. Wolf, R. Renner, T. C. Schäfer, B. Hupp, A. Steffen and M. Finze, *Angew. Chem.*, 2016, **128**, 10663–10667.
11. G. M. Sheldrick, *Acta Crystallogr.*, 2008, **A64**, 112–122.
12. G. M. Sheldrick, Universität Göttingen, 1997.
13. G. M. Sheldrick, Universität Göttingen, 2014.
14. G. M. Sheldrick, Universität Göttingen, 1997.
15. A. L. Spek, *Acta Crystallogr.*, 2009, **D65**, 148–155.
16. A. L. Spek, Utrecht University, Utrecht, The Netherlands, 2010.
17. L. J. Farrugia, University of Glasgow, 1995-2013.
18. C. B. Hübschle, G. M. Sheldrick and B. Dittrich, *J. Appl. Crystallogr.*, 2011, **44**, 1281–1284.
19. K. Brandenburg, Crystal Impact GbR, Bonn, Germany, 1997-2018.
20. D. Wu, A. Chen and C. S. Johnson Jr., *J. Magn. Reson. A* 1995, **115**, 260–264.
21. A. Einstein, *Ann. Phys.*, 1906, **19**, 289–306.
22. A. Einstein, *Ann. Phys.*, 1906, **19**, 371–381.
23. M. Sharma and S. Yashonath, *J. Phys. Chem. B*, 2006, **110**, 17207–17211.
24. A. Gierer and K. Wirtz, *Z. Naturforsch., A: Phys. Sci.*, 1953, **8**, 532–538.
25. H.-C. Chen and S.-H. Chen, *J. Phys. Chem.*, 1984, **88**, 5118–5121.
26. D. Zuccaccia and A. Macchioni, *Organometallics*, 2005, **24**, 3476–3486.
27. F. Neese, *WIREs Comput. Mol. Sci.*, 2012, **2**, 73-78.
28. J. P. Perdew, K. Burke and M. Ernzerhof, *Phys. Rev. Lett.*, 1996, **77**, 3865-3868.
29. J. P. Perdew, M. Emzerhof and K. Burke, *J. Chem. Phys.*, 1996, **105**, 9982-9985.
30. J. P. Perdew, K. Burke and M. Ernzerhof, *Phys. Rev. Lett.*, 1997, **78**, 1396-1396.
31. C. Adamo and V. Barone, *J. Chem. Phys.*, 1999, **110**, 6158-6170.
32. M. Ernzerhof and G. E. Scuseria, *J. Chem. Phys.*, 1999, **110**, 5029-5036.
33. J. M. Tao, J. P. Perdew, V. N. Staroverov and G. E. Scuseria, *Phys. Rev. Lett.*, 2003, **91**.
34. J. P. Perdew, J. M. Tao, V. N. Staroverov and G. E. Scuseria, *J. Chem. Phys.*, 2004, **120**, 6898-6911.
35. A. Schafer, H. Horn and R. Ahlrichs, *J. Chem. Phys.*, 1992, **97**, 2571-2577.
36. F. Weigend and R. Ahlrichs, *Phys. Chem. Chem. Phys.*, 2005, **7**, 3297-3305.
37. S. Grimme, J. Antony, S. Ehrlich and H. Krieg, *J. Chem. Phys.*, 2010, **132**.
38. S. Grimme, S. Ehrlich and L. Goerigk, *J. Comput. Chem.*, 2011, **32**, 1456-1465.
39. L. Laaksonen, *J. Mol. Graphics*, 1992, **10**, 33-34.
40. D. L. Bergman, L. Laaksonen and A. Laaksonen, *J. Mol. Graph. Model.*, 1997, **15**, 301-306.